





DUDLEY KNOX LIBRARY  
NAVAL POSTGRADUATE SCHOOL  
MONTEREY, CALIFORNIA 93943-6002









# NAVAL POSTGRADUATE SCHOOL

Monterey, California



## THESIS

ANALYSIS OF COMBUSTION OF  
A POROUS MEDIUM

by

Do Sung Park

December 1985

Thesis Advisor:

David Salinas

Approved for public release; distribution is unlimited

T226751





## REPORT DOCUMENTATION PAGE

a. REPORT SECURITY CLASSIFICATION Unclassified			1b. RESTRICTIVE MARKINGS		
a. SECURITY CLASSIFICATION AUTHORITY			3 DISTRIBUTION/AVAILABILITY OF REPORT Approved for public release; distribution is unlimited		
b. DECLASSIFICATION/DOWNGRADING SCHEDULE			5. MONITORING ORGANIZATION REPORT NUMBER(S)		
c. PERFORMING ORGANIZATION REPORT NUMBER(S)			7a. NAME OF MONITORING ORGANIZATION Naval Postgraduate School		
a. NAME OF PERFORMING ORGANIZATION Naval Postgraduate School		6b. OFFICE SYMBOL (If applicable) Code 69	7b. ADDRESS (City, State, and ZIP Code) Monterey, California 93943-5100		
c. ADDRESS (City, State, and ZIP Code) Monterey, California 93943-5100		8b. OFFICE SYMBOL (If applicable)	9. PROCUREMENT INSTRUMENT IDENTIFICATION NUMBER		
a. NAME OF FUNDING/SPONSORING ORGANIZATION		10 SOURCE OF FUNDING NUMBERS			
c. ADDRESS (City, State, and ZIP Code)		PROGRAM ELEMENT NO	PROJECT NO	TASK NO	WORK UNIT ACCESSION NO
f. TITLE (Include Security Classification) ANALYSIS OF COMBUSTION OF A POROUS MEDIUM					
g. PERSONAL AUTHOR(S) Park, Do S.					
a. TYPE OF REPORT Master's Thesis		13b TIME COVERED FROM TO		14 DATE OF REPORT (Year, Month, Day) 1985, December	15 PAGE COUNT 61
h. SUPPLEMENTARY NOTATION					
COSATI CODES			18. SUBJECT TERMS (Continue on reverse if necessary and identify by block number)		
FIELD	GROUP	SUB-GROUP	Porous Media; Combustion; Analytical Model; Transient; Heat Transfer		
ABSTRACT (Continue on reverse if necessary and identify by block number)					
<p>A numerical analysis of a heat transfer and combustion model for a porous medium within a circular cylinder is carried out. The basic mechanisms considered in the theory are: a carbon energy conservation equation, energy balance on the air, and an oxygen mass balance equation. Heat transfer mechanisms included in the model are conduction, convection, and radiation. A heat generation term arising from combustion of the carbon is included in the model. Transport mechanisms for oxygen mass transfer are molecular diffusion and convective transport. The governing heat and mass transfer equations are solved numerically by the Galerkin formulation of the Finite Element Method. The results show the effects</p>					
2. DISTRIBUTION/AVAILABILITY OF ABSTRACT <input checked="" type="checkbox"/> UNCLASSIFIED/UNLIMITED <input type="checkbox"/> SAME AS RPT <input type="checkbox"/> DTIC USERS			21. ABSTRACT SECURITY CLASSIFICATION Unclassified		
22. NAME OF RESPONSIBLE INDIVIDUAL Prof. David Salinas			22b TELEPHONE (Include Area Code) (408) 646-3426	22c OFFICE SYMBOL Code 69zc	

#19 - ABSTRACT - (CONTINUED)

of permeability, porosity, geometry and initial condition on the behavior of the system.

Approved for public release; distribution is unlimited.

Analysis of Combustion of a Porous Medium

by

Do Sung Park  
Lcdr, Republic of Korea Navy  
B.S., Korea Naval Academy, 1975

Submitted in partial fulfillment of the  
requirements for the degree of

MASTER OF SCIENCE IN MECHANICAL ENGINEERING

from the

NAVAL POSTGRADUATE SCHOOL

December 1985

## ABSTRACT

A numerical analysis of a heat transfer and combustion model for a porous medium within a circular cylinder is carried out. The basic mechanisms considered in the theory are: a carbon energy conservation equation, energy balance on the air, and an oxygen mass balance equation. Heat transfer mechanisms included in the model are conduction, convection, and radiation. A heat generation term arising from combustion of the carbon is included in the model. Transport mechanisms for oxygen mass transfer are molecular diffusion and convective transport. The governing heat and mass transfer equations are solved numerically by the Galerkin formulation of the Finite Element Method. The results show the effects of permeability, porosity, geometry and initial condition on the behavior of the system.

## TABLE OF CONTENTS

I.	INTRODUCTION -----	12
II.	DESCRIPTION OF THE PROBLEM -----	21
III.	NUMERICAL CONSIDERATIONS -----	28
IV.	DISCUSSION AND CONCLUSIONS -----	31
	A. EFFECTS OF POROSITY AND PERMEABILITY -----	31
	B. EFFECTS OF HEAT FLUX -----	44
	C. EFFECTS OF BOUNDARY CONDITIONS -----	49
	D. EFFECTS OF GEOMETRY -----	51
	E. CONCLUSIONS AND RECOMMENDATIONS -----	53
	APPENDIX: BOUNDARY CONDITIONS -----	55
	LIST OF REFERENCES -----	58
	INITIAL DISTRIBUTION LIST -----	60



## LIST OF TABLES

I.	POROSITY AND PERMEABILITY -----	33
II.	POROSITY AND PERMEABILITY FOR FIGURE 4.7 -----	43
III.	POROSITY AND PERMEABILITY FOR FIGURE 4.8 -----	46

## LIST OF FIGURES

2.1	Geometric Model of Porous Medium -----	22
3.1	Grid Convergence for the Finite Element Method ---	29
4.1	Carbon Temperature Profile with $d/D = 1.0$ and Constant Porosity ( $p = 0.476$ ) -----	34
4.2	Oxygen Concentration Profile with $d/D = 1.0$ and Constant Porosity ( $p = 0.476$ ) -----	35
4.3	Carbon Temperature Profile with $d/D = 0.75$ and Constant Porosity ( $p = 0.779$ ) -----	36
4.4	Oxygen Concentration Profile with $d/D = 0.75$ and Constant Porosity ( $p = 0.779$ ) -----	37
4.5	Carbon Temperature and Oxygen Concentration vs. Time for Varying $d/D$ ratios -----	38
4.6	Carbon Temperature vs. $z/z$ for Varying Time -----	39
4.7	Carbon Temperature and Oxygen Concentration vs. Time for Varying Permeabilities -----	42
4.8	Carbon Temperature and Oxygen Concentration vs. Time for Varying Porosities -----	45
4.9	Carbon Temperature Profile with Varying Heat Flux -----	47
4.10	Oxygen Concentration Profile with Varying Heat Flux -----	48
4.11	Carbon Temperature and Oxygen Concentration vs. Time for a Changing Boundary Condition -----	50
4.12	Carbon Temperature and Oxygen Concentration vs. Time for Varying the Axial Length of the Cylinder -----	52

## LIST OF SYMBOLS

A	-	Arrhenius coefficient, wetted surface area
$\tilde{A}$	-	Stiffness matrix
$\tilde{B}$	-	Mass matrix
C	-	Specific heat at constant pressure
D	-	Unit cell dimension
$\mathcal{D}$	-	Mass diffusion coefficient
d	-	Particle diameter
E	-	Activation energy
e	-	Specific internal energy
F	-	Fraction
$\tilde{F}$	-	Excitation vector
f	-	Stoichiometric ratio
G	-	Pseudo mass velocity
g	-	Gravitational constant
$\Delta H$	-	Heat of combustion
h	-	Convection heat transfer coefficient
K	-	Constant
k	-	Thermal Conductivity
L	-	Thickness of porous medium
$\ell_e$	-	Element length
M	-	Molecular weight
m	-	Specific permeability
n	-	Reaction order

$N_j$	- Global Basis Function
$P$	- Pressure
$Pr$	- Prandtl number
$p$	- Porosity
$Q$	- Filter velocity
$q$	- Heat generation or loss
$q'$	- Heat flux
$R$	- Reaction rate
$R'$	- Rate per unit area
$R$	- Gas constant
$Re$	- Reynolds number
$r$	- Radial coordinate
$R_i$	- Residual function
$T$	- Temperature
$\hat{T}$	- Absolute temperature
$t$	- Time
$t_{n-1}^*$	- Previous time step
$U$	- Internal energy
$u$	- Pore velocity, radial
$v$	- Pore velocity, axial
$V$	- Void volume, molecular volume
$z$	- Axial coordinate
$Z$	- Specific internal area

#### Greek Symbols

$\alpha$	- Thermal diffusivity
$\delta$	- Pore diameter

$\delta^k$	- Kronecker delta function
$\epsilon$	- Thermal emissivity
$\theta$	- Solution coefficient
$\wedge$	- Field operator
$\mu$	- Dynamic viscosity
$\xi$	- Local element coordinate
$\rho$	- Mass density
$\sigma$	- Stefan-Boltzman constant
$\tau$	- Tortuosity, stress
$\phi$	- Oxygen concentration
$\psi$	- Particle shape factor, approximate solution

### Subscripts

a	- Air
c	- Carbon
CO	- Carbon monoxide
CO <sub>2</sub>	- Carbon dioxide
e	- Effective
fm	- Film
g	- Heat generation
i	- At the current time or step
ig	- Ignition
o	- Cylinder dimension (i.e., $r_o$ is cylinder radius, $z_o$ is cylinder length)
O <sub>2</sub>	- Oxygen
P	- At constant pressure
r	- Radiation



s - Solid  
st - Starting  
u - Universal  
 $\infty$  - Ambient conditions

## I. INTRODUCTION

Combustion of porous media has far-reaching practical consequences. As there are large reserves of available coal in many places, coal combustion is a potential source of increased energy production if some of the pollution problems can be resolved. The combustion of coal is also useful for the heating of homes and buildings. On the other hand, undesirable combustion of matter in the form of fires causes great losses in lives and property destruction every year.

In order to gain the most advantage from its beneficial uses, and to minimize its destructive power, a clear understanding of combustion behavior is necessary. Among the various engineering disciplines, combustion is one of the least understood. The combustion problem is especially difficult because of its multi-disciplinary nature, involving the areas of fluid mechanics, heat transfer and chemical kinetics. Chemical kinetics of combustion is a most complex subject in itself, and the difficulty is compounded by the additional complications introduced by the other disciplinary areas.

Because of its importance, however, the area of combustion has been the subject of much investigation, both analytically and experimentally. In a 1973 survey paper, Emmons [Ref. 1] points out that the three major obstacles in the study of fires are turbulence, the immensely intricate chemistry, and the lack

of knowledge of the physical parameters dependence on temperature and composition. Emmons discusses the essential role of heat and mass transfer in fires, and points out that the conservation laws of mass, energy, and momentum must be supplemented by many other facts and laws accounting for chemistry, gas and liquid diffusion, mutual diffusion of gases, radiation effects, and the variation of thermodynamic, chemical, kinetic, transport, radiative and mechanical properties over the fire temperature range. Nevertheless Emmons asserts "Now is the time to take a new look, to detect and analyze the simpler parts of a fire, and thus open up the future of rational approaches."

Emmons points out that inclusion of the complete chemistry in a model would be overwhelming even if it were known, and that only that chemistry which is essential to the problem be included in the formulation. A brief summary of several "simpler" problems provides some insight into the overall problem.

In a 1936 paper, Parker and Hottel [Ref. 2], presented the results of an experimental study on the combustion of carbon. This fundamental investigation considered cylindrical carbon specimens combusting in air. They determined the distribution of  $N_2$ ,  $CO$ ,  $CO_2$ , and  $O_2$  in the gaseous "film" surrounding the carbon at varying ambient temperatures and air velocities. Resulting combustion temperatures varied between 1000 K and 1500 K (725°C to 1225°C, 1340°F to 2240°F). Results show that the partial pressure of  $CO$  decreases with distance from the

carbon surface, while the partial pressure of  $O_2$  increases with distance from the carbon surface. At a fixed temperature, the partial pressure of  $O_2$  at the carbon surface increased with increasing air velocity; while at fixed velocity the partial pressure of oxygen decreased with increasing temperature. Additionally, a separate experiment measured combustion rate as a function of temperature and air velocity. Their results show that at constant velocity, the reaction rate increases with increasing temperature; and the reaction rate increases with increasing velocity when the temperature is held constant. The experiments demonstrated that there is little CO at the carbon surface at the higher temperatures. An equation for the reaction rate of carbon brush is presented. The denominator of this equation contains two additive terms, namely, the diffusional resistance  $R_d$  and the chemical resistance  $R_c$ . With increasing temperature,  $R_c$  decreases and the combustion is diffusion controlled; when the velocity increases,  $R_d$  decreases and the combustion is kinetically controlled.

In a 1951 paper, Arthur [Ref. 3] presents the results of an experimental investigation of the combustion of two carbons of widely different reactivities in the temperature range of 735-1175 K (460-900°C, 860-1650°F). The study shows that two reactions occur; one leads to  $CO_2$  formation and the other to CO formation. It was shown that 1) the rate of carbon gasification decreases but slightly with carbon consumption, 2) the combustion temperatures increase with air flow rate,

3) the  $\text{CO}/\text{CO}_2$  ratio increases with temperature, with  $\text{CO}/\text{CO}_2$  about 8.2 at 1105 K (834°C, 1533°F) and 11.1 at 1168 K (895°C, 1645°F), 4) the gasification rate is independent of air flow rate at low temperatures and increases rapidly at higher temperatures (the transition occurred at 595 K for carbon A, and 993 K for carbon B), and 5) the  $\text{CO}/\text{CO}_2$  ratio was independent of the initial partial pressure of oxygen. The most significant result is that in the 673 K to 1173 K temperature range, the  $\text{CO}/\text{CO}_2$  ratio increases exponentially with temperature from 1% at 673 K to 12% at 1173 K.

In a 1956 investigation, Koizumi [Ref. 4] conducted an experimental and analytical study of combustion of solid fuels in fixed beds. He found 1) that the oxidation zone is only one or two partical diameters deep from the burning front, 2) that the burning rate is controlled by the rate of gas diffusion in the boundary layer (i.e., the chemical reation occurs instantaneously, and 3) that the CO to  $\text{CO}_2$  combustion occurs in the boundary layer.

In 1961, Green and Perry [Ref. 5] presented the results of an analytical investigation of heat transfer with a flowing fluid through a porous medium. They formulated a one-dimensional transient model including conduction and convection. The fluid flow rate was assumed constant, and the thermophysical properties were assumed to be independent of temperature. Two coupled p.d.e. were obtained from energy balances on the solid (porous media), and the flowing fluid. Boundary conditions



were taken as equal fluid and solid temperatures at  $X = 0$ , and  $X \rightarrow \infty$ . The initial condition was taken as equal fluid and solid temperatures for all  $X$ . The p.d.e. were solved by the finite-difference method. They found that heat conduction and convection are both important for internal Reynolds numbers less than unity; and that the fluid and solid temperatures are essentially the same when the dimensionless parameter  $(hz/k_f)^{1/2} \cdot (k_f/p_f c_f u)$  is greater than 0.342.

In a 1974 paper, Anderson and Zienkiewicz [Ref. 6] presented an analytical investigation of a reactive solid with zero order kinetics. Two problems were considered: the steady state problem, and the transient problem. In the steady state problem, the Frank-Kamenetski parameter is determined. This parameter indicates whether combustion will occur or not. In the transient case, the body is immersed in a thermal field whose temperature is greater than the ignition temperature of the body. Here the time to ignition (i.e., the induction time) is determined, as well as transient solutions  $T(x,y,t)$  of two-dimensional bodies. The problem is solved by the Galerkin finite element method. Although the formulation permits variable conductivity and specific heats, the authors assume these parameters constant in their illustrative examples. A single nonlinear p.d.e. obtained by an energy balance, includes conduction and convection heat transfer models.

In a 1976 paper, Kim and Chung [Ref. 7] presented the results of an analytical investigation of conditions leading

to a state of self-sustaining combustion in a porous medium. The one-dimensional transient model includes combustion and conduction. Two p.d.e. were obtained from an energy and mass balance of the porous medium. Thermophysical property dependence on temperature was not accounted for. Laplace's asymptotic method was used to obtain a solution. Solid gas reactions are considered to occur volumically throughout the porous medium. A constant rate of oxidant fuel is assumed at  $X = 0$ . Zero gradients of temperature and oxidant concentration at  $X \rightarrow \infty$  were taken as boundary conditions. The boundary conditions at  $X = 0$  are  $-\lambda \partial T / \partial X = \dot{q}$  and  $-D \partial C / \partial X = \dot{m}$ . Their results for a semi-infinite slab show that ignition is strongly dependent upon temperature and reactant concentration. The Lewis number was taken as unity. They also show that as either the activation energy decreases or the initial temperature of the porous medium increases, the ignition occurs faster.

In 1976, Sawyer and Shuck [Ref. 8] presented a transient, one-dimensional model for underground coal gasification of a coal bed with vertical micro fissures along which combustion occurs. Mass and energy balance for the solid and gas phases, and mass balance equation for each species (oxygen, carbon monoxide, and carbon dioxide) leads to 7 coupled, nonlinear p.d.e. The heat transfer mechanisms include conduction in the solid, convection in the gas and convection between the solid and gas. All properties except permeability and reaction rates were assumed constant. The 7 p.d.e. are supplemented by an

equation of state for the gas, and a Darcy flow equation in the fissures. The system is solved by the finite-difference method.

Sahota and Pagni [Ref. 9] present the results of an analytical investigation of heat and mass transfer in porous media subject to fires in a 1978 paper. The one-dimensional transient model includes conduction and convection. Energy and mass conservation equations, together with species conservation equations, Darcy's law and state equations lead to 8 equations which are solved by the finite difference method. A portion of the domain has initial moisture. The energy balance includes a heat sink term to account for the evaporation of water. Thermophysical properties are treated as constants. When pressures are not required, a simplified technique for determining temperature has been developed. The method neglects heat transfer by convection and mass diffusion. This analysis is valid when very small air vapor mixture velocity is present, and for very small Lewis numbers (i.e., when  $C_n U_m \ll 1$  and  $C_m L_e \ll 1$ ).

In a 1980 paper, Saatdjian and Caltergironi [Ref. 10] presented a mathematical model for a plane porous matrix bounded by two impermeable surfaces. The porous matrix is composed of a mixture of nonreacting fiber glass and a resin which decomposes exothermically into gaseous products as the matrix temperature increases. The two-dimensional transient model includes conduction, convection and combustion, but does not

account for temperature dependent properties. The fluid is modelled as a perfect gas, and flow through the porous matrix is governed by Darcy's law. It is assumed that the matrix properties remain unchanged during the reaction (i.e., the fiber fraction/resin remains greater than 0.90), and the gaseous products and the fluid which initially filled the enclosed region are the same. The density of the saturating gas is allowed to vary. Results show temperature and density as functions of time. The problem couples the effects of two phenomena, convective movement and chemical reaction. As the reaction is depleted, natural convection alone subsists.

In a 1981 paper, Chan and Banejess [Ref. 11] investigated transient three-dimensional natural convection in porous media. The model includes a continuity equation, two momentum equations and two energy balance equations. The finite difference method solves the five p.d.e.'s for the solid and fluid temperatures, the velocity components in the X and Y directions, and the pressure. The method uses upwind differencing for the advective term. This model allows for unequal solid and fluid temperatures. The authors state that the solid and fluid temperatures are equal ("equal diffusivity" model) when the filtration velocity is not too high and both phases are well dispersed. Fictitious conductivities take into account the dispersed structure of the solid matrix and the effect of hydrodynamic dispersion in the fluid energy balance equation. The porous medium is modelled as an assembly of spheres.

The authors introduce a scheme to reduce diffusional truncation errors. Analytical results show good agreement with experimental results for Rayleigh numbers between 36 and 800. Numerical results at higher Rayleigh numbers deviate from experimental results. The model predicts convective instabilities at high Rayleigh numbers.

In a 1981 paper, Hickox [Ref. 12] presented an investigation into convective flow, induced by a heat source, through a porous medium of low permeability. The two-dimensional transient model includes conduction and convection. Four equations are obtained: an equation of continuity, Darcy's law for fluid flow, an energy balance on the porous medium and a state equation. The problem arises, for example, when a container of radioactive waste material is deposited in a sea bed below the sedimentary layer. The Boussinesq approximation that density changes are due only to buoyancy is used. Permeability, viscosity, thermal conductance, thermal capacity and the thermal expansion coefficient are treated as constants. Numerical solutions based on similarity transformations were obtained for steady state point and line sources, as well as a steady state, constant temperature sphere. The results are predicted to be accurate for Reynolds numbers less than unity. In the case of the subseabed porous medium, a Reynolds number of 10 is anticipated. The analysis is valid only for distances a few canisters away from the disposed canister.



## II. DESCRIPTION OF THE PROBLEM

This investigation considers the combustion of a porous graphite medium. The porous medium is constructed from graphite particulate matter, either in the form of spherical particles or cylindrical fibers, imbedded in a cylindrical container. We assume the porous medium has a regular periodic structure with interconnecting pores which permit the flow of air through the medium. Figure 2.1 shows a geometric model of a regular periodic structure.

Initially the porous medium is at ambient conditions. It is then subjected to a heat source at the bottom of the vertical container for a specified period of time. Upon termination of the heat flux, the system is at a greater temperature (and lower oxygen concentration) than the ambient temperature. Thereafter the system temperature will either decrease to ambient temperature, or it will continue to burn at higher temperature. The former process leads to extinction, the latter process is combustion. Which of these processes occurs depends on the particular attributes of the system such as its porosity, permeability, thickness and other distinguishing properties. This investigation seeks to determine how combustion of the porous graphite medium is related to the properties of the medium.

The air which flows through the porous medium has two effects: it supplies oxygen for combustion which produces

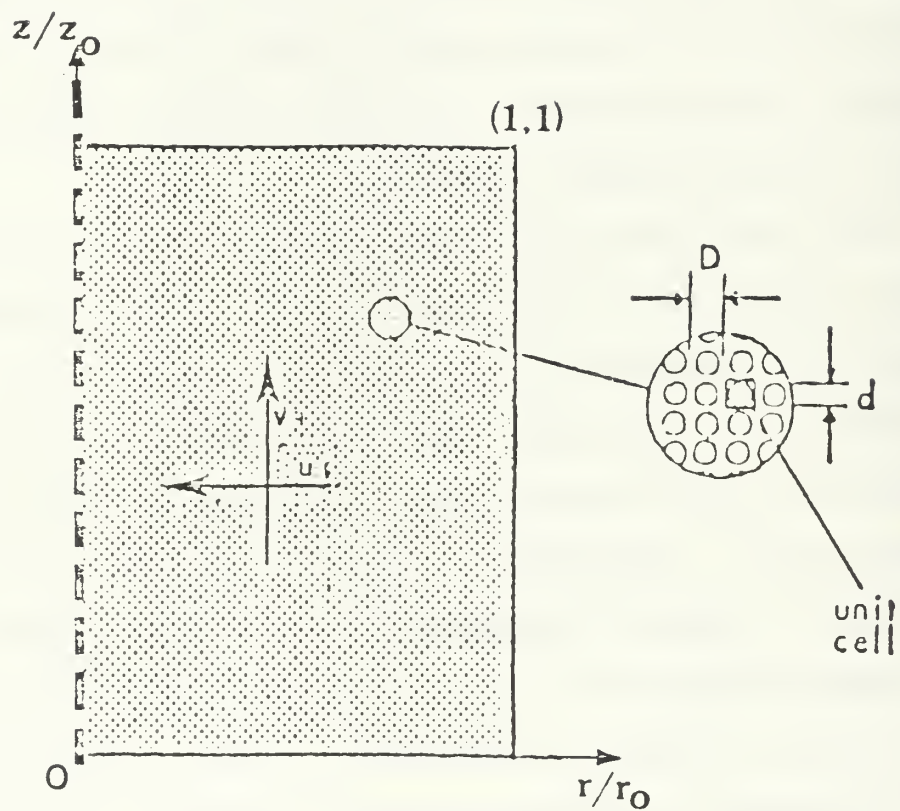


Figure 2.1 Geometric Model of Porous Medium

heat, and it provides for convective heat transfer through the medium. Combustion occurs if the heat generation of combustion is the dominant effect. If the heat transfer is the dominant effect, then extinction will occur. Which of these effects dominates depends upon the physical system under consideration, as well as the boundary and initial conditions.

The mathematical model is formulated in the following way. We assume the air flow through the porous medium is governed by Darcy's law. Previous investigation has shown that the Darcy law model is an excellent approximation when the Reynolds number is less than 1. This occurs for the flow through the porous media covered in this investigation. In any case, that Reynolds number is less than one must be verified from the results of the analysis. The use of Darcy's law obviates the conservation of momentum equations. This results in a very significant simplification of the mathematical model, with a corresponding reduction of computational effort.

Energy balance on the porous solid, and on the air flowing through the porous solid yield two heat transfer equations. These heat transfer equations include conduction, and convection mechanisms. In addition the porous solid energy equation includes a radiation term; and the air energy balance equation includes a term to account for the energy transport by flow. The porous solid energy balance equation also contains a heat generation term to account for the combustion of the

porous graphite. This term is obtained as the product of the reaction rate and enthalpy of formation. Both energy balance equations have a term reflecting the change in internal energy. We note, in passing, that the independent variables are the spatial cylindrical coordinates  $r$  and  $z$ , and the time coordinate  $t$ . The dependent variables are the temperatures of the porous graphite  $T_g$ , and the air flowing through the medium  $T_a$ . In addition the heat generation term in the porous solid energy balance equation introduces another dependent variable, the oxygen concentration, into the equation.

The third field equation is obtained by a mass balance of oxygen. This oxygen transport equation includes a molecular diffusion term, a convective transport term and a term to account for oxygen consumption due to combustion. This last term is obtained as the product of the reaction rate and the inverse of the stoichiometric ratio of the reaction. Diffusion due to temperature and pressure gradients were assumed to be negligible.

Finally a fourth field equation was obtained by combining Darcy's law for flow with the continuity equation. This equation introduces pressure as the fourth field variable.

The above description is a brief summary and is not complete in and of itself. Each of the individual terms in each of the field equations must be modeled in their own right. For example, there is a model for the diffusion coefficient of oxygen into air; there is a model for the effective

conductivity parameter for the porous solid, and so on. This investigation did not develop each of these models, and therefore the interested reader can obtain details of all of the models in the original developments of Vatikiotis [Ref. 12] and Martinez [Ref. 13].

For the sake of completeness, a brief description of the combustion and chemical kinetic models follows. The essential ideas of the combustion model were presented by N.N. Semenov [Ref. 14]. Semenov's model proposes that the combustion process occurs in two phases, the kinetic regime, and the diffusion regime. The initial combustion at lower temperatures is called the kinetic regime because there is sufficient oxygen present for combustion to proceed and the reaction is controlled by the actual kinetics of the surface reaction and does not depend on the diffusion rate. In the kinetic regime, the reaction rate increases, exponentially with temperature. As the temperature increases, the reaction rate increases and the rate of oxygen consumption increases; causing a lack of oxygen for further increase in the reaction. In this case, the lack of oxygen slows down the reaction. This regime of combustion, whereby the reaction rate is limited by the diffusion of oxygen is known as the diffusion regime. A graph of reaction rate versus temperature results in the well-known S-curve. The lower portion of the S-curve defines the kinetic regime; the upper portion of the S-curve defines the diffusion regime.



The chemical kinetics of combustion is much too complex to model all chemical reactions in detail. Instead, an approximate model was used whereby we assumed that the products of graphite combustion were only carbon monoxide and carbon dioxide. Empirical results by other investigations have proposed such models. In the present work, the model proposed by Arthur [Ref. 3] was taken. This model presents an expression which relates the ratio of CO and CO<sub>2</sub> to the temperature of the reaction.

The expression used for the reaction rate itself, is of the Arrhenius type. However, in accordance with the remarks of Frank-Kamenetskii [Ref. 15], the order of the reaction was not set to unity. Frank-Kamenetskii proposed that a fractional order reaction between 1/3 and 2/3 is a better representation of the experimental data of Parker and Hottel [Ref. 2]. This parameter was left to the selection of the investigator. It should be noted that combustion analyses show that significant changes in the system behavior occur with small changes in the reaction order.

The final mathematical model consists of four transient field equations in the four unknowns: graphite temperature, air temperature, oxygen concentration and pressure. These partial differential equations are both coupled and nonlinear. Together with boundary and initial conditions, these equations form a well-posed problem which cannot be solved exactly. An approximate solution was obtained by transforming the set of



4 p.d.e. into a system of ordinary differential equations using a Galerkin formulation of the finite element method. Details of the finite element formulation can be found in [Ref. 13].

### III. NUMERICAL CONSIDERATIONS

A Galerkin formulation of the finite element method was used to obtain solutions of the porous medium and air energy equations, the oxygen diffusion equation, and the continuity equation.

A grid arrangement as shown in Figure 3.1, which has 7 non-uniform divisions in the  $r$ -direction and 14 non-uniform divisions in the  $z$ -direction, was selected. The  $z$ -direction divisions were smaller near the  $z/z_0 = 0.0$ , where the carbon temperature and oxygen concentration change rapidly. The  $r$ -direction divisions were uniform in the middle, and non-uniform at the two ends  $r/r_0 = 0.0$  and  $r/r_0 = 1.0$ , where the carbon temperature and oxygen concentration change slightly. The  $r$  and  $z$  grid lines are as follows:

$r/r_0$ : 0.000, 0.125, 0.250, 0.500, 0.750, 0.875,  
1.000

$z/z_0$ : 0.000, 0.001, 0.0025, 0.005, 0.0075, 0.010,  
0.015, 0.020, 0.0500, 0.100, 0.2500, 0.500,  
0.750, 1.000

The results obtained from this grid compared very well (within 5% at all nodal points) with results obtained by a finer  $14 \times 14$  grid, and therefore the  $7 \times 14$  grid was used for all computer analyses.

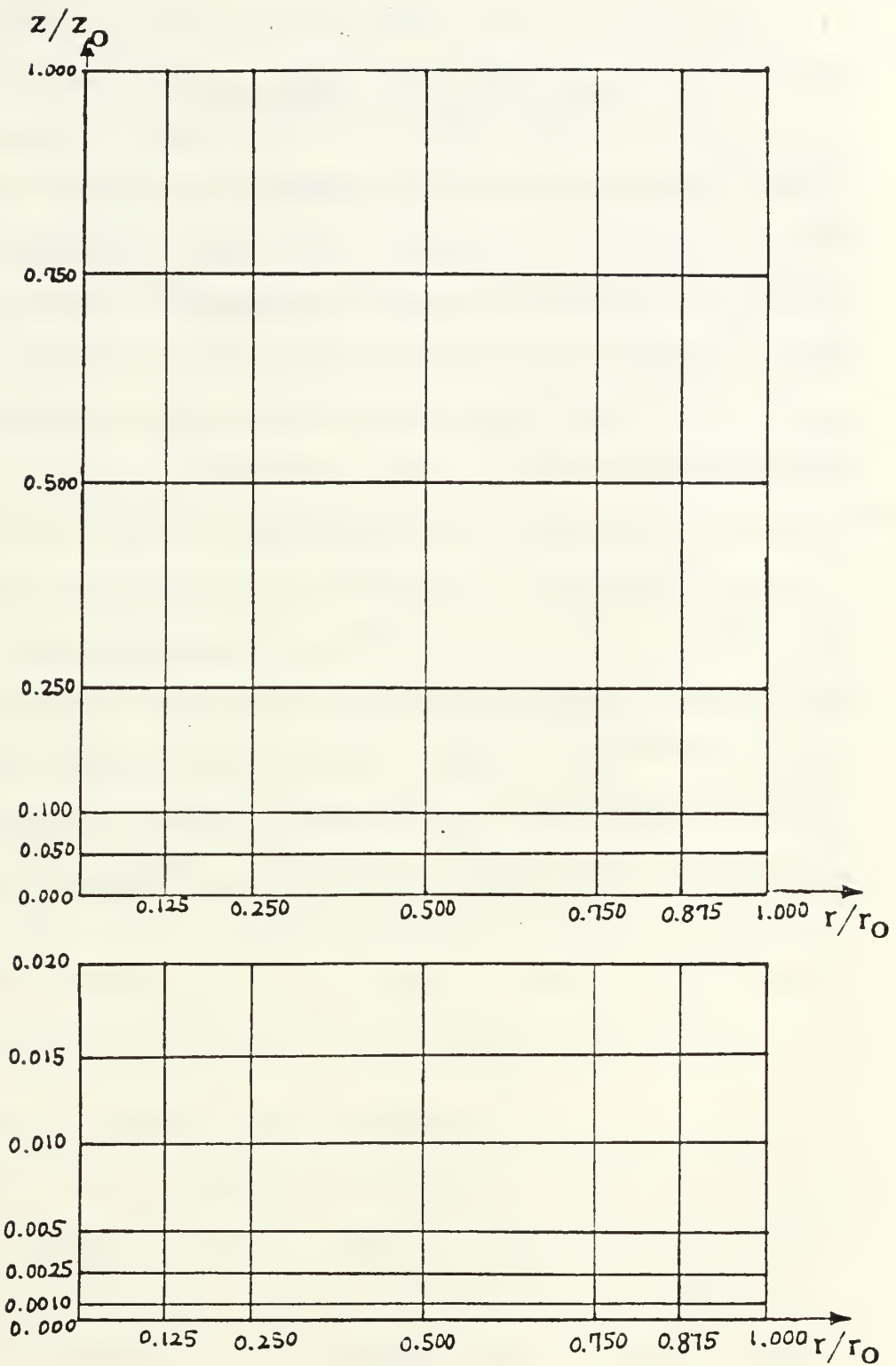


Figure 3.1. Grid Convergence for the Finite Element Method

The inputs for the integration program include (1) initial time step, (2) minimum time step, (3) maximum time step, and (4) property up-date time. The selection of these parameters affects the accuracy of the numerical solution. However, it is not possible to determine the error associated with any particular selection of these parameters. The selection of these parameters is by trial and error. If they're made very "small" the program runs very slowly and meaningful results could be very computationally expensive to obtain. If these parameters are selected too "large" the program may give poor results or it may not run at all. For this program, the initial time step is  $10^{-6}$  hr, the minimum time step is  $10^{-9}$  hr, the maximum time step is 0.25 hr, and the up-date time is  $10^{-14}$  hr. If the initial time step and the up-date time is larger than a certain time interval, the program overflows or underflows in subprogram NUITSL and LDASUB.

#### IV. DISCUSSION AND CONCLUSIONS

A heat transfer and combustion model for a porous medium within a cylinder is considered. The assumption of the model is that of the idealized porous medium described in Chapter III. The results of this investigation are intended to describe the behavior of a porous carbon medium with a heat generation term. The behavior of the temperature and oxygen concentration of the system depends upon the initial conditions, the boundary conditions, the geometry of the system, the porosity, the permeability, and the heat flux. A number of analyses were performed to determine how some of these parameters affect the system behavior. The boundary conditions for the investigations of Sections A, B, C, and D are presented in the Appendix. The porous media was initially at a constant temperature of 100 degrees Fahrenheit, a constant oxygen concentration of  $0.0172 \text{ lbm/ft}^3$  (ambient conditions), and a constant pressure of  $2118.7 \text{ lbf/ft}^2$  (14.7 psi).

##### A. EFFECTS OF POROSITY AND PERMEABILITY

Section IV.A.1 presents the results of varying  $d/D$  ratios (Table I, Figures 4.1-4.6). Section IV.A.2 changes  $D$  and  $d$ , keeping the porosity constant, with varying permeability (Table II, Figure 4.7). In Section IV.A.3, the  $d/D$  ratio is varied so that permeability is constant and porosity is changing (Table III, Figure 4.8).

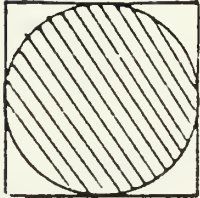
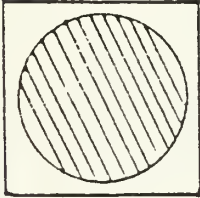
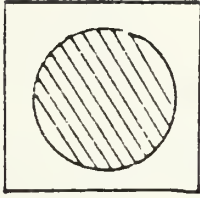
## 1. Effects of the d/D Ratio

In this section the effects of porosity and permeability on system behavior were investigated. Varying the carbon diameter, all other parameters fixed, results in changes to both the porosity and the permeability. Table I shows the three values selected for the carbon diameter and the resulting values of porosity and permeability. The results of this investigation are shown in Figures 4.1-4.6. In all investigations in this section a heat flux of  $500 \text{ Btu/ft}^2\text{-hr}$  was applied for 30 minutes and then turned off. Figures 4.1 and 4.2 show the temperature and oxygen concentration profile with  $d/D = 1.0$ . Figures 4.3 and 4.4 show the temperature and oxygen concentration with  $d/D = 0.75$ . Figure 4.5 compares the carbon temperature and oxygen concentration as a function of time, at the position  $r/r_0 = 0.5$  and  $z/z_0 = 0.0$ , for the three sets of  $d/D$  ratios. Figure 4.6 shows how the carbon temperature varies with the  $z$ -coordinate axis and time, at  $r/r_0 = 0.5$ .

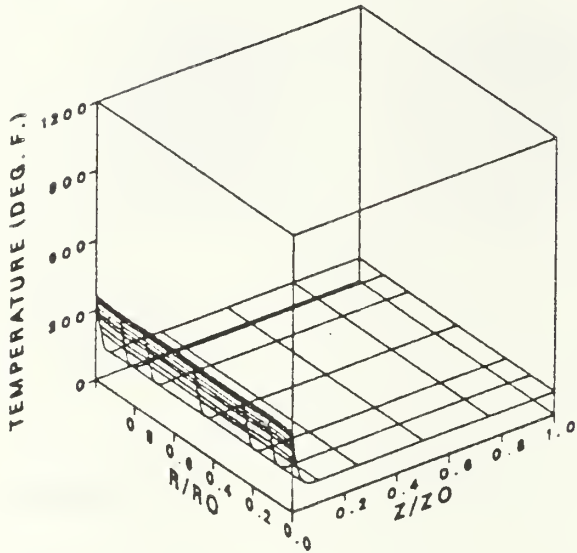
As shown in Figures 4.1-4.4, the  $d/D$  ratio affects the carbon temperature and oxygen concentration. These figures show that these variables are essentially independent of the radial direction, as they should be for the boundary conditions of these problems. Figures 4.1 and 4.2 show that at 12.2 minutes and  $z/z_0 = 0.0$ , the carbon temperature is 480 degrees Fahrenheit, and the oxygen concentration has not changed because the temperature is too low. However, we note that the



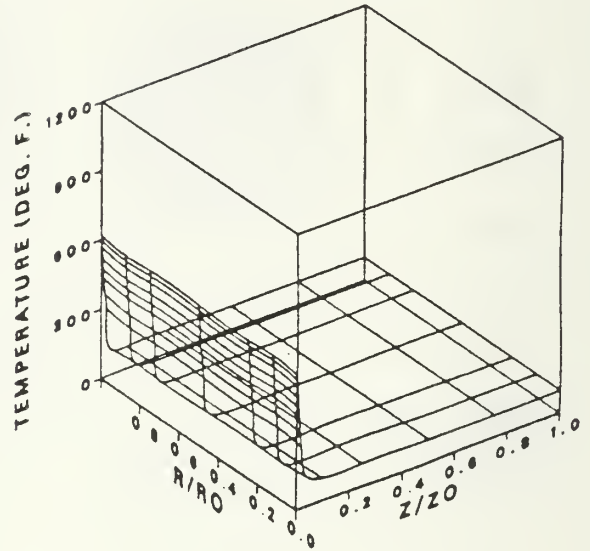
TABLE I  
POROSITY AND PERMEABILITY

shape			
	$d/D = 1.0$	$d/D = 0.875$	$d/D = 0.75$
Unit Cell Dimension (ft)	0.000417	0.000417	0.000417
Particle Diameter (ft)	0.000417	0.000365	0.000313
Porosity	0.476	0.649	0.779
Pore Diameter (ft)	$5.059 \times 10^{-4}$	$9.005 \times 10^{-4}$	$1.471 \times 10^{-3}$
Specific Internal Area (1/ft)	3766.9	2884.0	2118.9
Permea- bility (ft <sup>2</sup> )	$6.464 \times 10^{-10}$	$2.797 \times 10^{-9}$	$8.959 \times 10^{-9}$

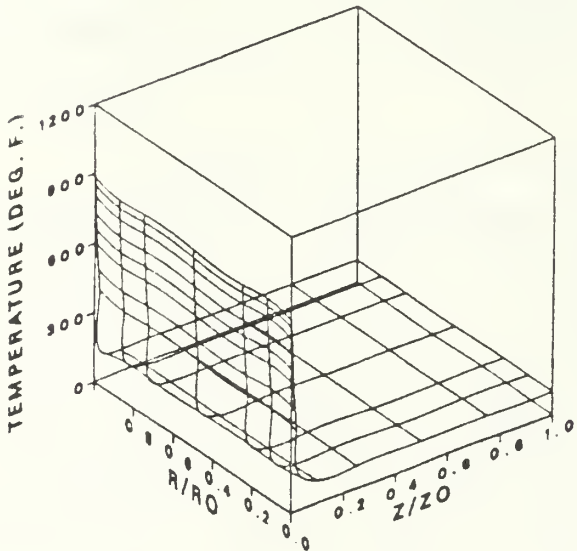
CARBON TEMPERATURE SURFACE  
 PROBLEM TIME IS 5.20 MIN.  
 HEAT FLUX AT  $Z/Z_0 = 500$ . BUT/FT<sup>2</sup>-HR.  
 $R_0 = 1.00$  FT.  
 $Z_0 = 1.00$  FT.  
 $T_{MAX} = 383$ . DEG. F.



CARBON TEMPERATURE SURFACE  
 PROBLEM TIME IS 5.10 MIN.  
 HEAT FLUX AT  $Z/Z_0 = 1000$ . BUT/FT<sup>2</sup>-HR.  
 $R_0 = 1.00$  FT.  
 $Z_0 = 1.00$  FT.  
 $T_{MAX} = 620$ . DEG. F.



CARBON TEMPERATURE SURFACE  
 PROBLEM TIME IS 5.00 MIN.  
 HEAT FLUX AT  $Z/Z_0 = 1500$ . BUT/FT<sup>2</sup>-HR.  
 $R_0 = 1.00$  FT.  
 $Z_0 = 1.00$  FT.  
 $T_{MAX} = 885$ . DEG. F.



CARBON TEMPERATURE SURFACE  
 PROBLEM TIME IS 4.20 MIN.  
 HEAT FLUX AT  $Z/Z_0 = 2000$ . BUT/FT<sup>2</sup>-HR.  
 $R_0 = 1.00$  FT.  
 $Z_0 = 1.00$  FT.  
 $T_{MAX} = 1091$ . DEG. F.

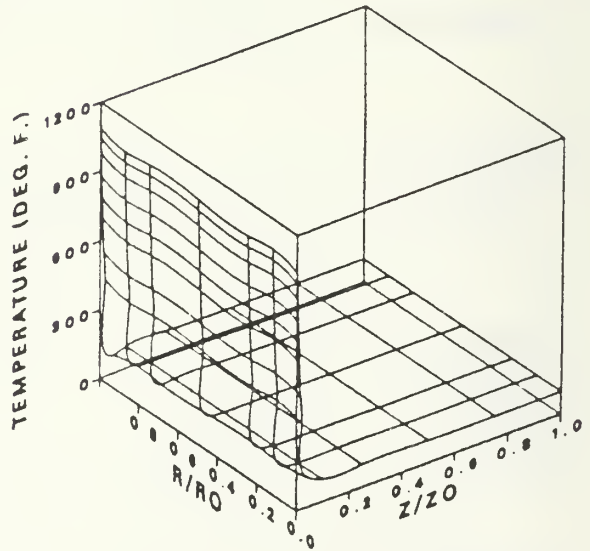
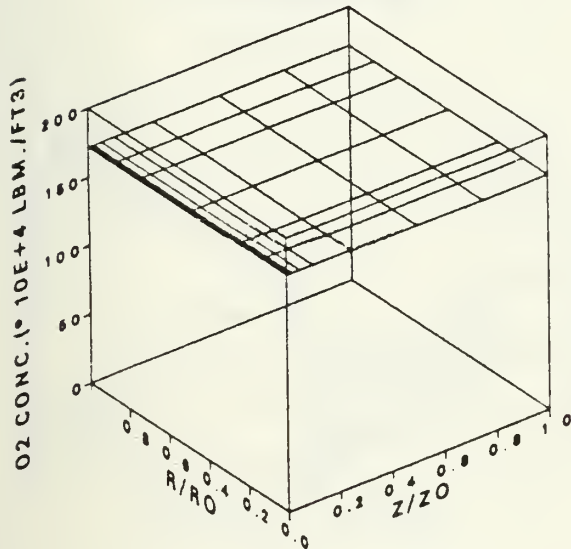
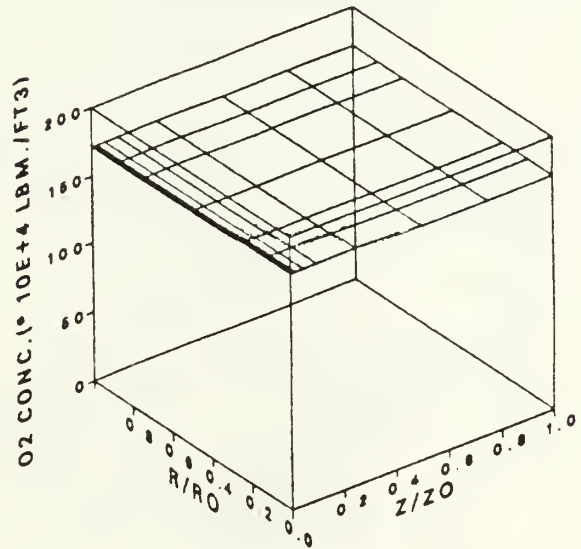


Figure 4.1 Carbon Temperature Profile with  $d/D = 1.0$  and constant porosity ( $p = 0.476$ )

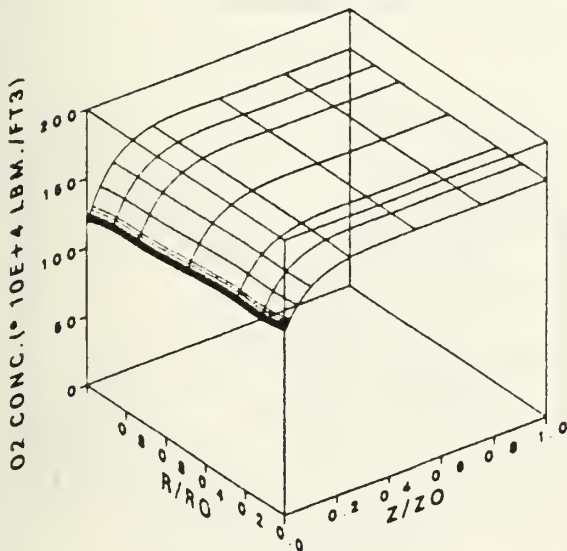
O<sub>2</sub> CONCENTRATION SURFACE  
 PROBLEM TIME IS 5.20 MIN.  
 HEAT FLUX AT Z/ZO = 500. BUT/FT<sup>2</sup>-HR.  
 RO = 1.00 FT.  
 ZO = 1.00 FT.  
 O<sub>2</sub> CONC, MIN = 172.



O<sub>2</sub> CONCENTRATION SURFACE  
 PROBLEM TIME IS 5.10 MIN.  
 HEAT FLUX AT Z/ZO = 1000. BUT/FT<sup>2</sup>-HR.  
 RO = 1.00 FT.  
 ZO = 1.00 FT.  
 O<sub>2</sub> CONC, MIN = 172.



O<sub>2</sub> CONCENTRATION SURFACE  
 PROBLEM TIME IS 5.00 MIN.  
 HEAT FLUX AT Z/ZO = 1500. BUT/FT<sup>2</sup>-HR.  
 RO = 1.00 FT.  
 ZO = 1.00 FT.  
 O<sub>2</sub> CONC, MIN = 119.



O<sub>2</sub> CONCENTRATION SURFACE  
 PROBLEM TIME IS 4.20 MIN.  
 HEAT FLUX AT Z/ZO = 2000. BUT/FT<sup>2</sup>-HR.  
 RO = 1.00 FT.  
 ZO = 1.00 FT.  
 O<sub>2</sub> CONC, MIN = 0.

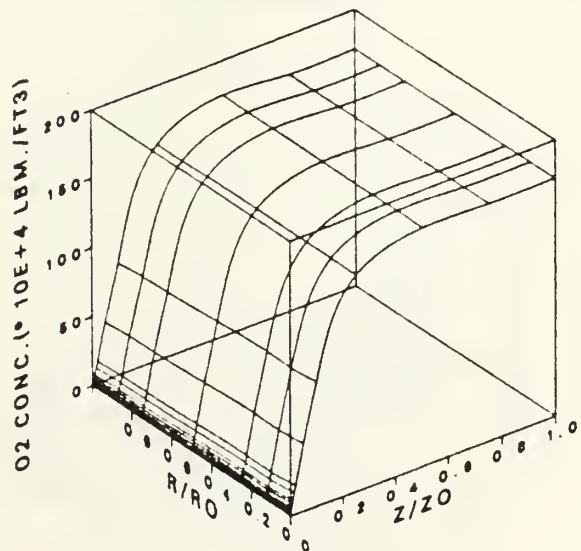
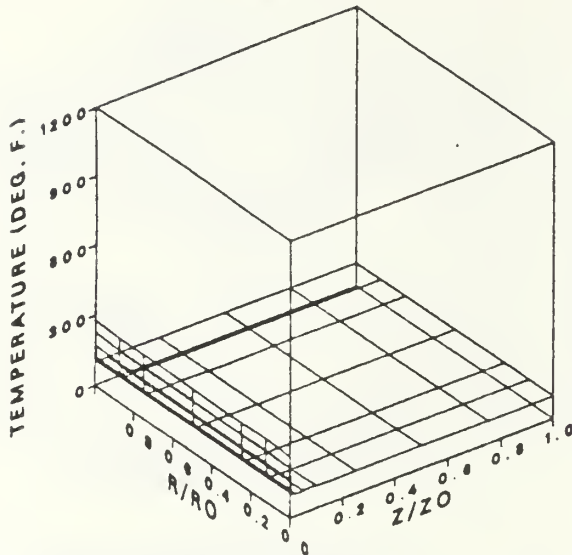
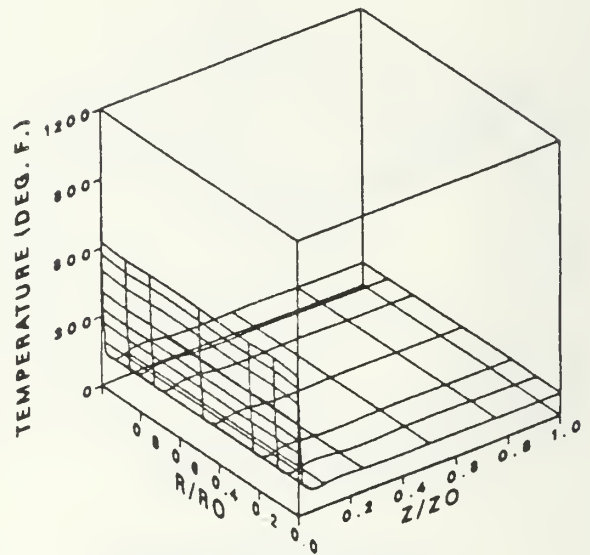


Figure 4.2 Oxygen Concentration Profile with  $d/D = 1.0$  and constant porosity ( $p = 0.476$ )

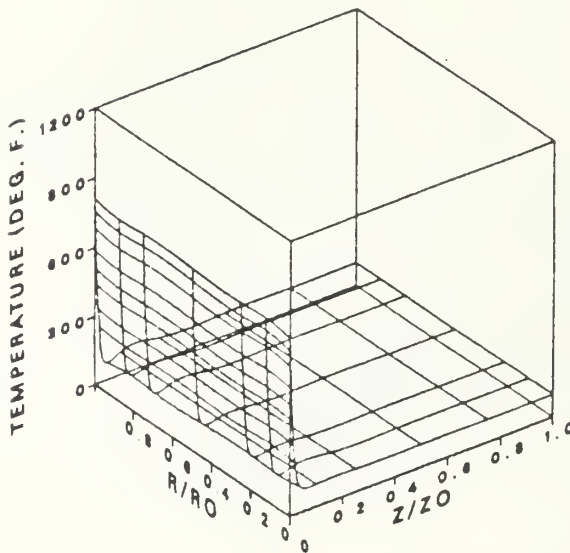
CARBON TEMPERATURE SURFACE  
 PROBLEM TIME IS 0.20 MIN.  
 HEAT FLUX AT  $Z/Z_0 = 500$ . BUT/FT<sup>2</sup>-HR.  
 $R_0 = 1.00$  FT.  
 $Z_0 = 1.00$  FT.  
 LITTLE  $d/D = 0.75$   
 $T_{MAX} = 278$ . DEG. F.



CARBON TEMPERATURE SURFACE  
 PROBLEM TIME IS 2.20 MIN.  
 HEAT FLUX AT  $Z/Z_0 = 500$ . BUT/FT<sup>2</sup>-HR.  
 $R_0 = 1.00$  FT.  
 $Z_0 = 1.00$  FT.  
 LITTLE  $d/D = 0.75$   
 $T_{MAX} = 627$ . DEG. F.



CARBON TEMPERATURE SURFACE  
 PROBLEM TIME IS 5.00 MIN.  
 HEAT FLUX AT  $Z/Z_0 = 500$ . BUT/FT<sup>2</sup>-HR.  
 $R_0 = 1.00$  FT.  
 $Z_0 = 1.00$  FT.  
 LITTLE  $d/D = 0.75$   
 $T_{MAX} = 812$ . DEG. F.



CARBON TEMPERATURE SURFACE  
 PROBLEM TIME IS 12.20 MIN.  
 HEAT FLUX AT  $Z/Z_0 = 500$ . BUT/FT<sup>2</sup>-HR.  
 $R_0 = 1.00$  FT.  
 $Z_0 = 1.00$  FT.  
 LITTLE  $d/D = 0.75$   
 $T_{MAX} = 1202$ . DEG. F.

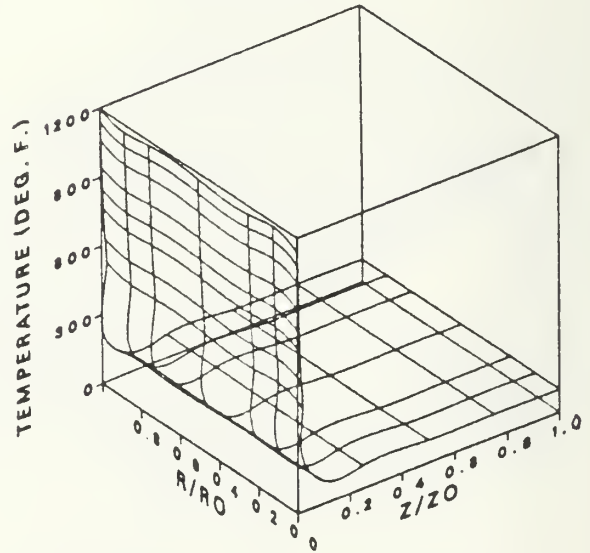
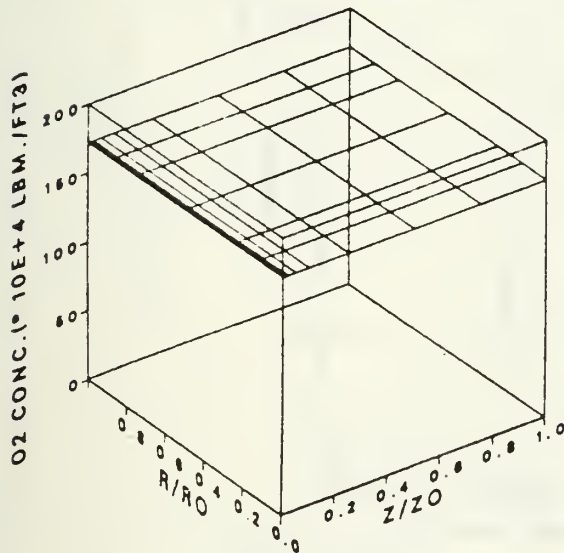
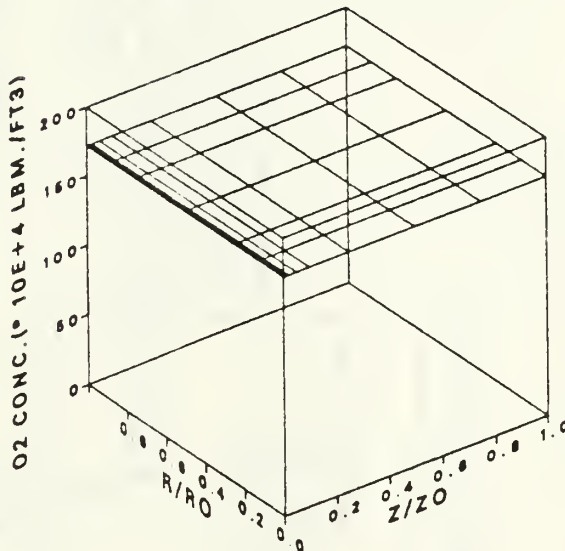


Figure 4.3 Carbon Temperature Profile with  $d/D = 0.75$  and constant porosity ( $p = 0.779$ )

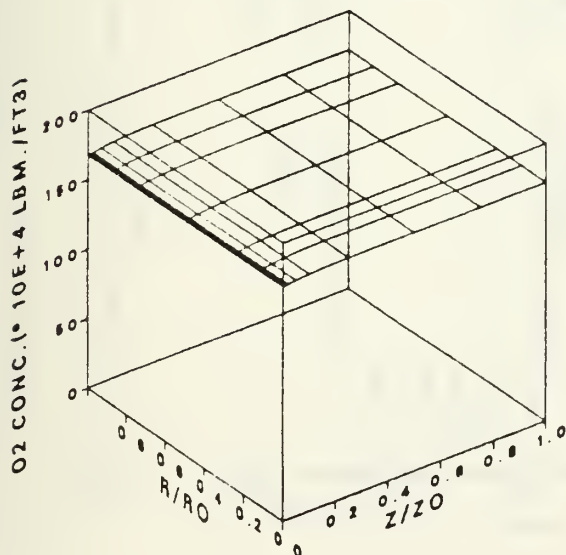
O2 CONCENTRATION SURFACE  
 PROBLEM TIME IS 0.20 MIN.  
 HEAT FLUX AT Z/ZO = 500. BUT/FT2-HR.  
 RO = 1.00 FT.  
 ZO = 1.00 FT.  
 LITTLE D/ BIG D = 0.75  
 O2 CONC, MIN = 172.



O2 CONCENTRATION SURFACE  
 PROBLEM TIME IS 2.20 MIN.  
 HEAT FLUX AT Z/ZO = 500. BUT/FT2-HR.  
 RO = 1.00 FT.  
 ZO = 1.00 FT.  
 LITTLE D/ BIG D = 0.75  
 O2 CONC, MIN = 172.



O2 CONCENTRATION SURFACE  
 PROBLEM TIME IS 5.00 MIN.  
 HEAT FLUX AT Z/ZO = 500. BUT/FT2-HR.  
 RO = 1.00 FT.  
 ZO = 1.00 FT.  
 LITTLE D/ BIG D = 0.75  
 O2 CONC, MIN = 167.



O2 CONCENTRATION SURFACE  
 PROBLEM TIME IS 12.20 MIN.  
 HEAT FLUX AT Z/ZO = 500. BUT/FT2-HR.  
 RO = 1.00 FT.  
 ZO = 1.00 FT.  
 LITTLE D/ BIG D = 0.75  
 O2 CONC, MIN = 0.

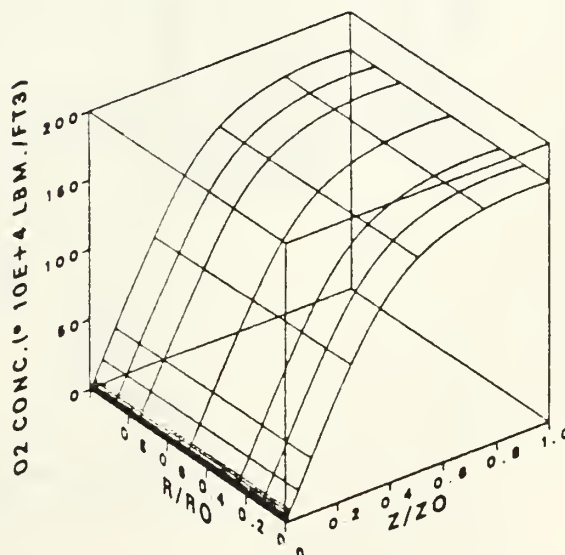


Figure 4.4 Oxygen Concentration Profile with  $d/D = 0.75$  and constant porosity ( $p = 0.779$ )



HEAT FLUX = 500 BTU/FT<sup>2</sup>-HR  
 POSITION ; R/RO = 0.5  
 Z/ZO = 0.0  
 INITIAL TEMP. = 100°F

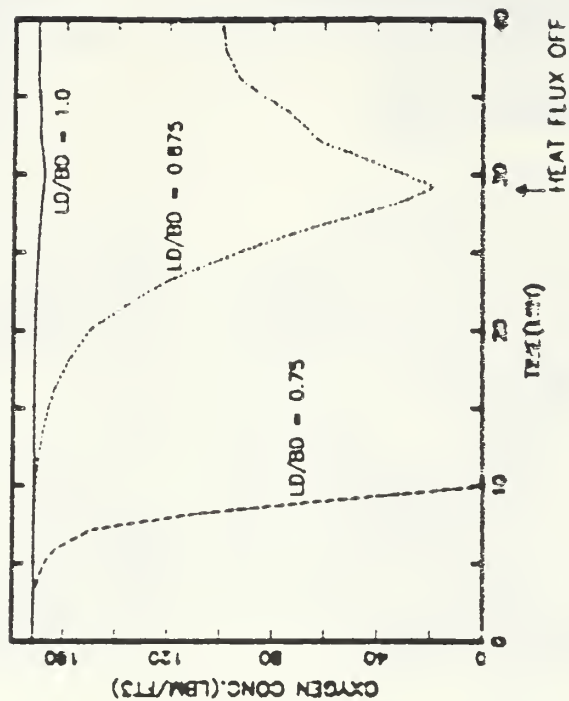
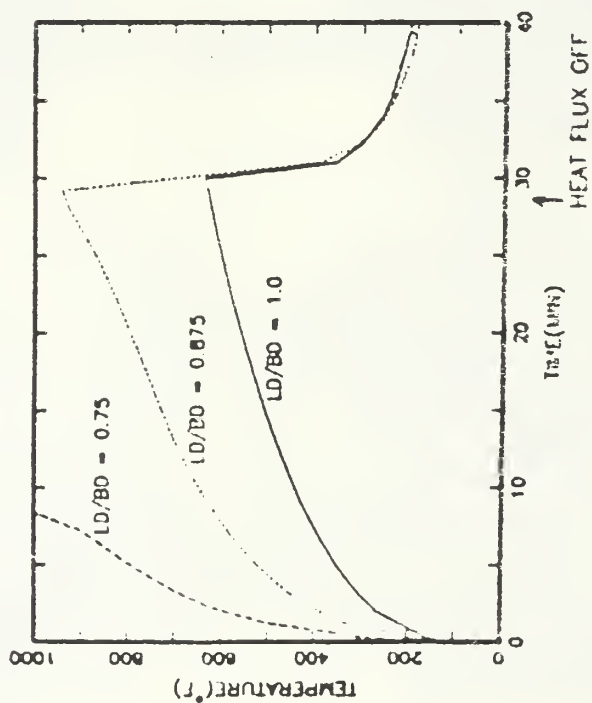


Figure 4.5 Carbon Temperature and Oxygen Conc. VS. Time  
 for varying d/D ratios



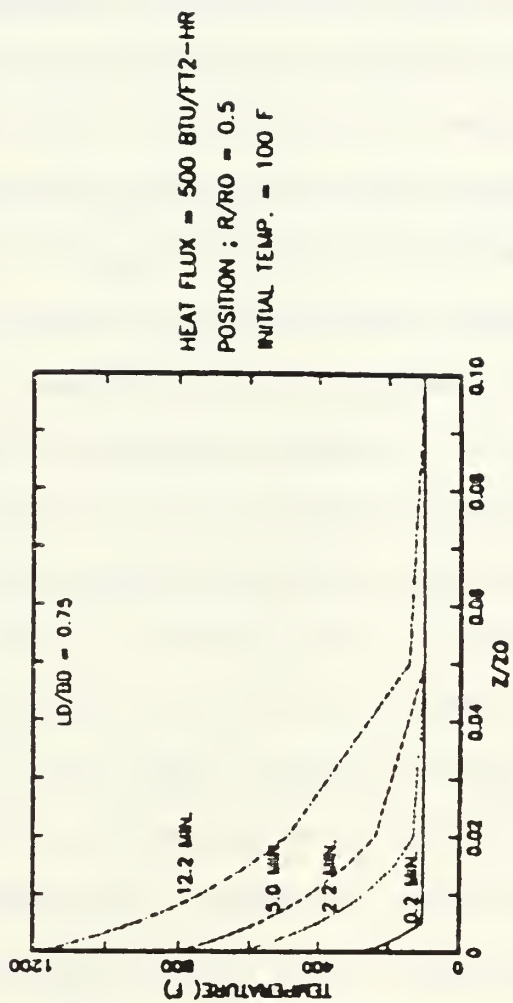
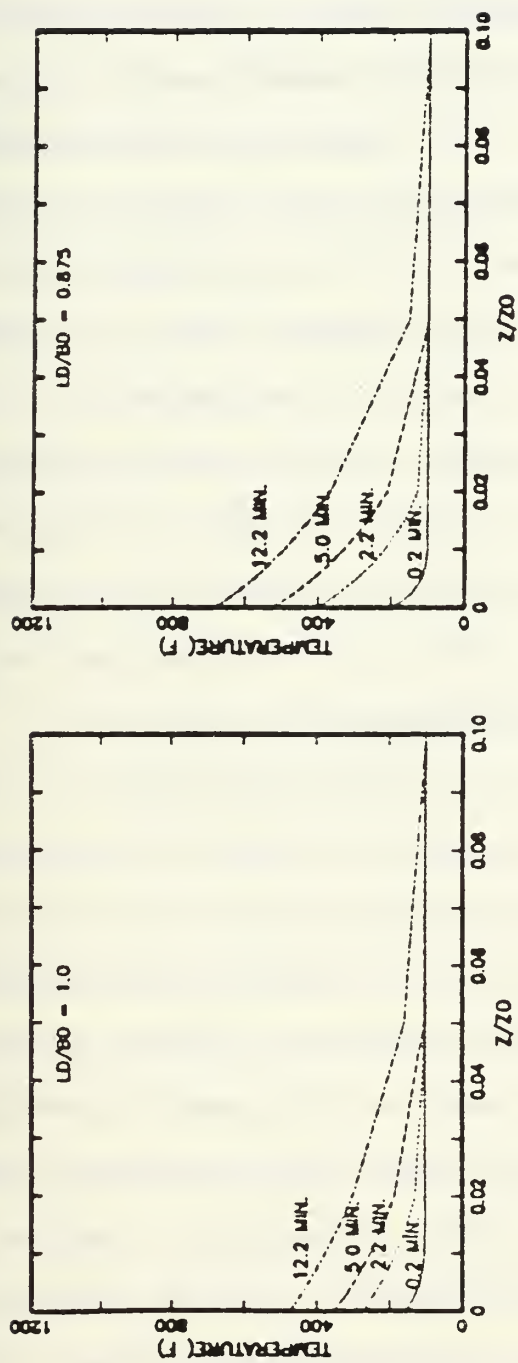


Figure 4.6 Carbon Temperature VS.  $z/z_0$  for Varying Time

temperature gradient is very large over a small region in the vicinity of the imposed heat flux. The region of temperature activity does not extend beyond  $z/z_0 = 0.1$ . Figures 4.3 and 4.4, with  $d/D = 0.75$ , show the carbon temperature and oxygen concentration. At  $z/z_0 = 0.0$  and 12.2 minutes, the carbon temperature is 1200 degrees Fahrenheit and the oxygen concentration becomes almost zero. The results show that combustion activity increases with decreasing  $d/D$ . This can be attributed to an increase in the air flow velocity.

Figure 4.5 shows the effect of  $d/D$  ratios on combustion activity at  $r/r_0 = 0.5$  and  $z/z_0 = 0.0$ . As shown in Figure 4.5, with  $d/D = 1.0$ , combustion activity is the least and the oxygen remains almost constant. With  $d/D = 0.875$ , combustion activity increases so that the oxygen is depleted at  $z/z_0 = 0.0$  in about 30 minutes. With  $d/D = 0.75$ , combustion activity becomes very strong resulting in a depletion of oxygen at  $z/z_0 = 0.0$  in about 10 minutes. The reason being that as the  $d/D$  ratio decreases, there is an increase in void space, which allows more oxygen to be supplied to the combustion region. Also, with a smaller  $d/D$ , the carbon mass per unit cell is smaller and therefore the heat flux per carbon mass increases. This results in an increase of the carbon temperature. In the case of  $d/D = 0.75$ , there was no opportunity to monitor behavior beyond 10 minutes because the program terminated due to numerical difficulties. For the other two cases of  $d/D = 0.875$  and 1.0, the heat flux was removed after 30 minutes to observe

whether the system would continue to combustion or go to extinction. The carbon temperatures dropped sharply and the porous carbon medium returned to its initial temperature while the oxygen concentration returned to its original concentration somewhat less sharply.

Figure 4.6 illustrates the behavior of carbon temperature versus  $z/z_o$  at  $r/r_o = 0.5$  as time is varied for each of the  $d/D$  ratios. These figures show that the carbon temperature is greatest at  $z/z_o = 0.0$ , and the carbon temperature approaches the constant ambient temperature as  $z/z_o$  increases. Thus in all cases we observe that combustion occurs in a local region near the base of the system where oxygen is entering into the medium.

## 2. Effects of Permeability

Figure 4.7 shows the carbon temperature and oxygen concentration as a function of time, at  $r/r_o = 0.5$  and  $z/z_o = 0.0$ , for various permeabilities with porosity fixed. The boundary conditions are the same as Section V.A.1 except that the heat flux was changed from 500 Btu/ft<sup>2</sup>-hr to 1000 Btu/ft<sup>2</sup>-hr. The description of the porous medium used in this investigation is shown in Table II. Porosities and  $d/D$  ratios are the same for cases A, B, C, and D. Case A has the smallest unit cell ( $D = 0.0002085$  ft), the smallest particle size, and the smallest permeability ( $6.993 \times 10^{-10}$  ft<sup>2</sup>); case D has the largest unit cell ( $D = 0.000834$  ft), the largest particle size, and the largest permeability ( $1.119 \times 10^{-8}$  ft<sup>2</sup>). Unfortunately

HEAT FLUX = 1000 BTU/FT<sup>2</sup>-HR  
 POSITION; R/RO = 0.5  
 Z/ZO = 0.0  
 INT. TEMP. = 100 F  
 POROSITY = 0.649

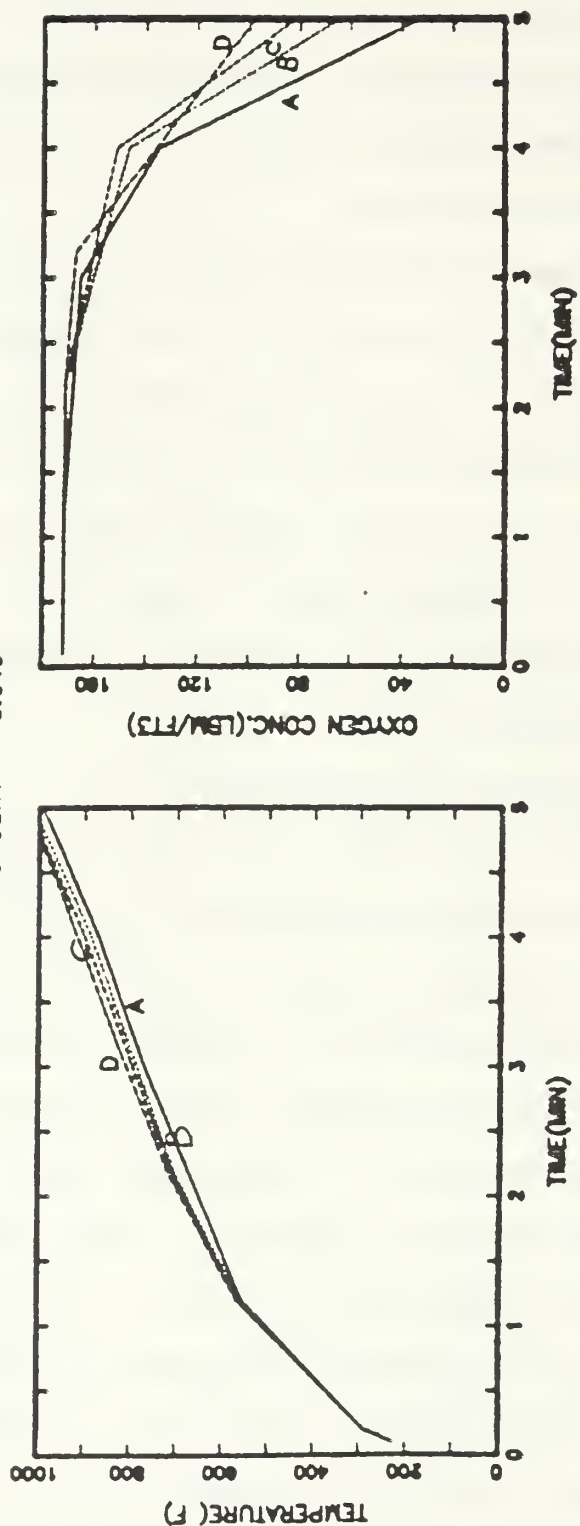


Figure 4.7 Carbon Temperature and Oxygen Conc. VS. Time  
 for Varying Permeabilities

TABLE II  
POROSITY AND PERMEABILITY FOR FIGURE 4.7

	Unit Cell Dimension (ft)	Particle Diameter (ft)	Ratio	Porosity	Permeability (ft <sup>2</sup> )
A	.0002085	.0001824	.875	0.6492	$6.993 \times 10^{-10}$
B	.000417	.0003649	.875	0.6492	$2.797 \times 10^{-9}$
C	.0006255	.0005473	.875	0.6492	$6.29 \times 10^{-9}$
D	.000834	.0007298	.875	0.6492	$1.119 \times 10^{-8}$

it was not possible to obtain analysis beyond  $t = 5$  minutes because the program has difficulty running when the oxygen concentration gets very small. The results show that as permeability increases, the carbon temperature slightly increases, while the oxygen concentration increases. This shows that an increase in permeability provides additional oxygen for a small enhancement of combustion.

### 3. Effects of Porosity

In this section the effects of porosity on system behaviors are investigated. Figure 4.8 shows the carbon temperature and the oxygen concentration, at  $r/r_o = 0.5$  and  $z/z_o = 0.0$ , as a function of time. The description of the porous medium used in this investigation is shown in Table III. Here porosity is the same for cases A and B, and cases C and D, while permeability is the same for cases A and C, and cases B and D. Figure 4.8 shows that for the same porosity (cases A and B, and cases C and D) carbon temperature and oxygen concentration are the same. For the same permeability, the carbon temperature and oxygen concentration have different values. It appears from these results that the carbon temperature and oxygen concentration are strongly affected by porosity and are not affected by permeability. This result is difficult to explain and may indicate an error in the program.

### B. EFFECTS OF HEAT FLUX

Figures 4.9 and 4.10 show the changes in carbon temperature and oxygen concentration as the heat flux is varied.



HEAT FLUX = 1000 BTU/FT<sup>2</sup>-HR  
 POSITION; R/RO = 0.5  
 Z/ZO = 0.0  
 INT. TEMP. = 100 F

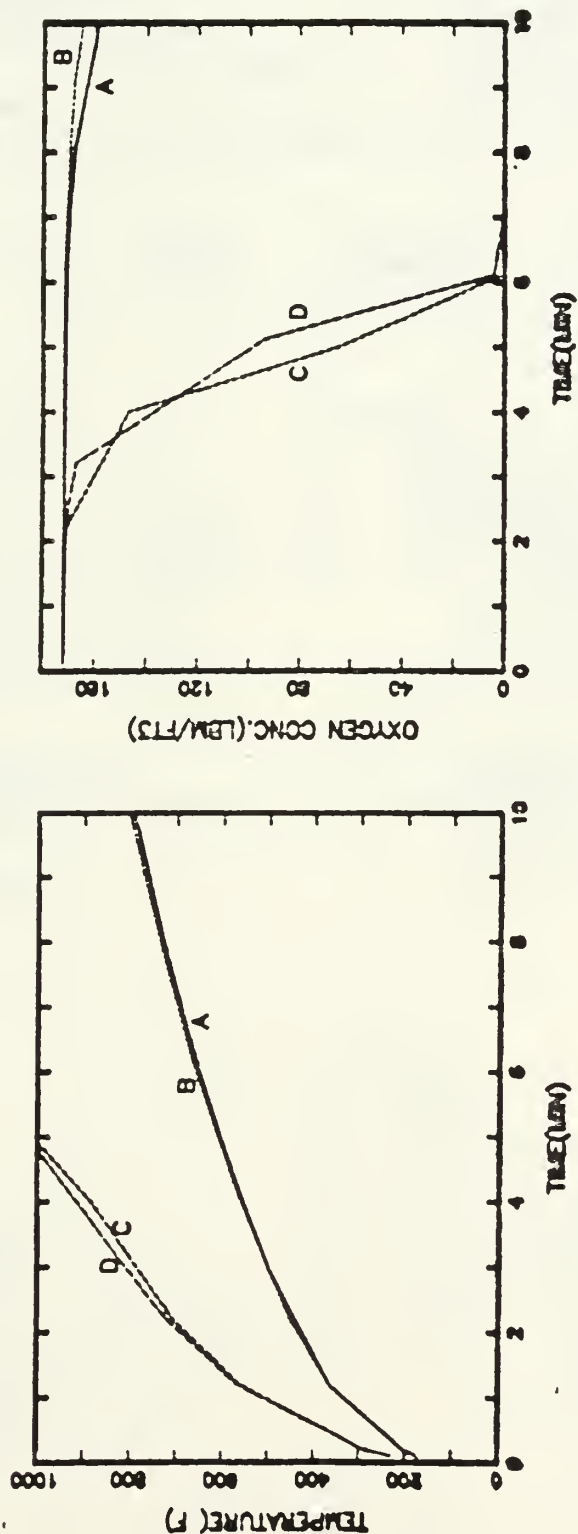


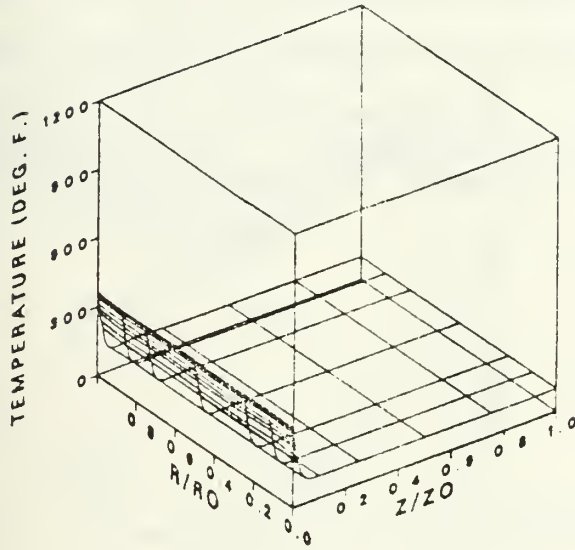
Figure 4.8 Carbon Temperature and Oxygen Conc. VS. Time  
 for Varying Porosities

TABLE III

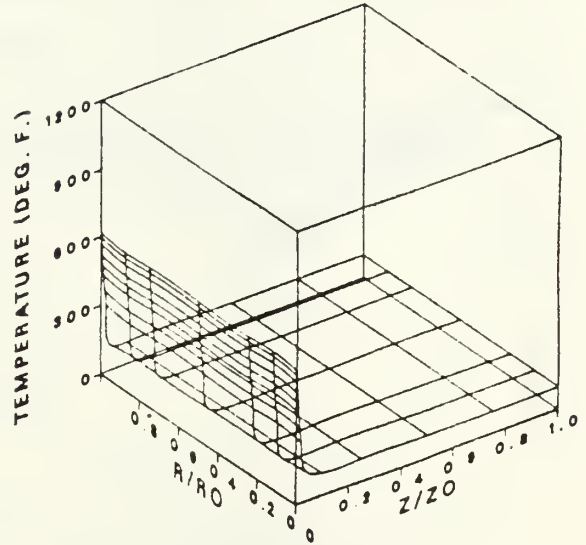
POROSITY AND PERMEABILITY FOR FIGURE 4.8

	Unit Cell Dimension (ft)	Particle Diameter (ft)	The d/D Ratio	Porosity	Permeability (ft <sup>2</sup> )
A	.000866	.000866	1.0	0.4764	$2.797 \times 10^{-9}$
B	.001733	.001733	1.0	0.4764	$1.119 \times 10^{-8}$
C	.000417	.000365	0.875	0.6492	$2.797 \times 10^{-9}$
D	.000834	.000730	0.875	0.6492	$1.119 \times 10^{-8}$

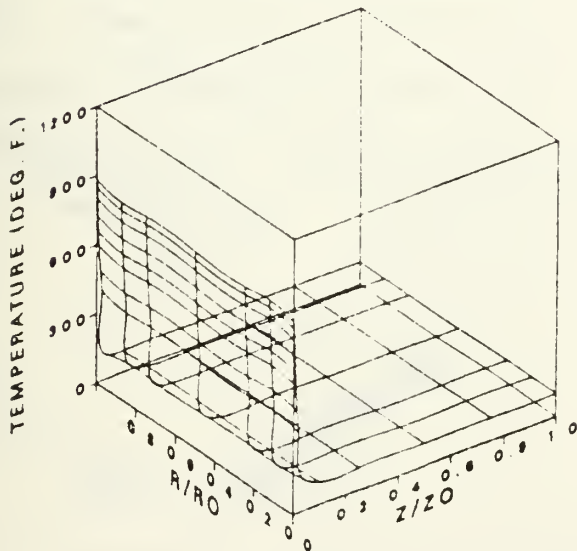
CARBON TEMPERATURE SURFACE  
 PROBLEM TIME IS 5.20 MIN.  
 HEAT FLUX AT  $Z/Z_0 = 500$ . BUT/FT<sup>2</sup>-HR.  
 $R_0 = 1.00$  FT.  
 $Z_0 = 1.00$  FT.  
 $T_{MAX} = 363$ . DEG. F.



CARBON TEMPERATURE SURFACE  
 PROBLEM TIME IS 5.10 MIN  
 HEAT FLUX AT  $Z/Z_0 = 1000$ . BUT/FT<sup>2</sup>-HR.  
 $R_0 = 1.00$  FT.  
 $Z_0 = 1.00$  FT.  
 $T_{MAX} = 620$ . DEG. F.



CARBON TEMPERATURE SURFACE  
 PROBLEM TIME IS 5.00 MIN  
 HEAT FLUX AT  $Z/Z_0 = 1500$ . BUT/FT<sup>2</sup>-HR.  
 $R_0 = 1.00$  FT.  
 $Z_0 = 1.00$  FT.  
 $T_{MAX} = 885$ . DEG. F.



CARBON TEMPERATURE SURFACE  
 PROBLEM TIME IS 4.20 MIN.  
 HEAT FLUX AT  $Z/Z_0 = 2000$ . BUT/FT<sup>2</sup>-HR.  
 $R_0 = 1.00$  FT.  
 $Z_0 = 1.00$  FT.  
 $T_{MAX} = 1091$ . DEG. F.

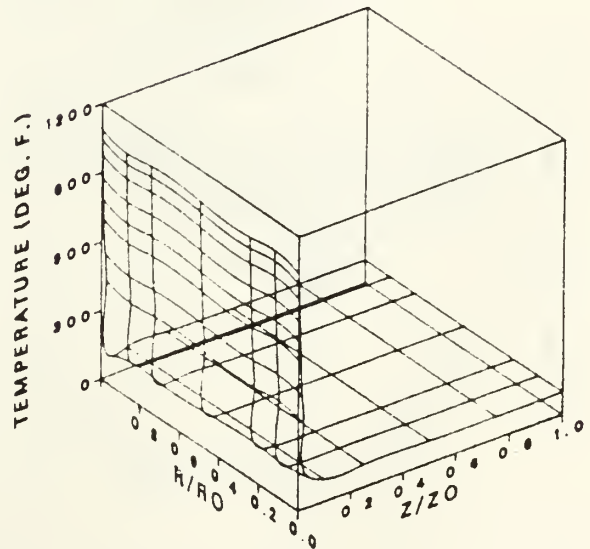
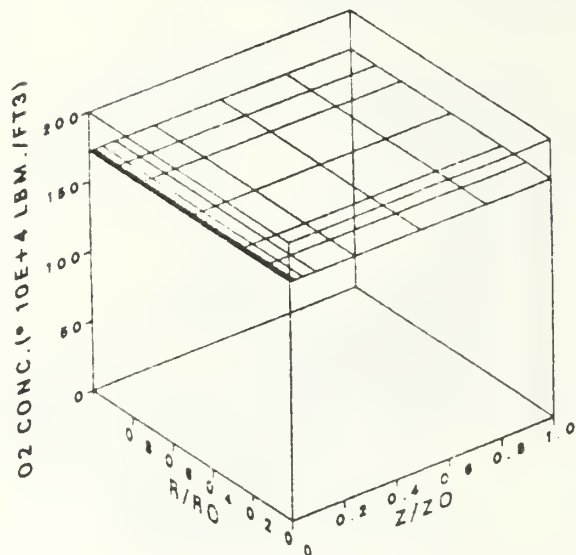
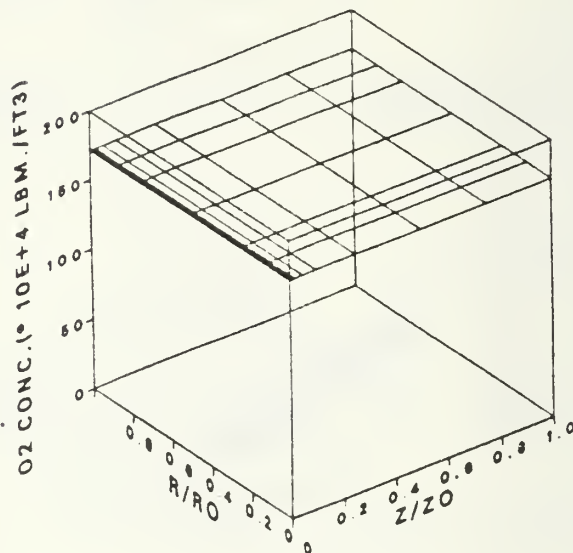


Figure 4.9 Carbon Temperature Profile  
 with Varying Heat Flux

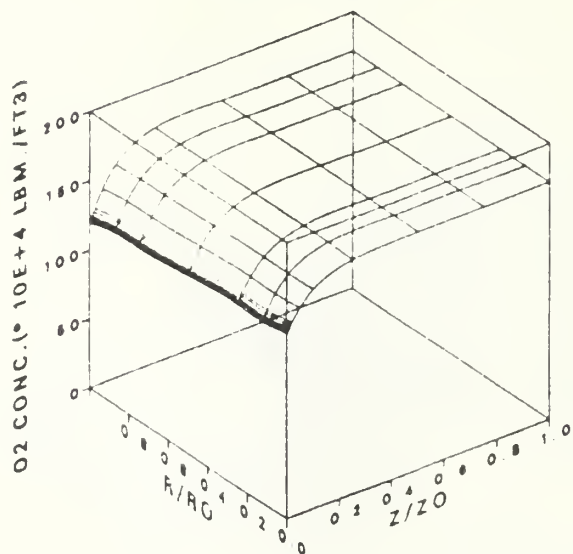
O2 CONCENTRATION SURFACE  
 PROBLEM TIME IS 5.20 MIN.  
 HEAT FLUX AT  $Z/Z_0 = 500$ . BUT/FT<sup>2</sup>-HR.  
 $R_0 = 1.00$  FT.  
 $Z_0 = 1.00$  FT.  
 O2 CONC, MIN = 172



O2 CONCENTRATION SURFACE  
 PROBLEM TIME IS 5.10 MIN.  
 HEAT FLUX AT  $Z/Z_0 = 1000$ . BUT/FT<sup>2</sup>-HR.  
 $R_0 = 1.00$  FT.  
 $Z_0 = 1.00$  FT.  
 O2 CONC, MIN = 172



O2 CONCENTRATION SURFACE  
 PROBLEM TIME IS 5.00 MIN.  
 HEAT FLUX AT  $Z/Z_0 = 1500$ . BUT/FT<sup>2</sup>-HR.  
 $R_0 = 1.00$  FT.  
 $Z_0 = 1.00$  FT.  
 O2 CONC, MIN = 119.



O2 CONCENTRATION SURFACE  
 PROBLEM TIME IS 4.20 MIN.  
 HEAT FLUX AT  $Z/Z_0 = 2000$ . BUT/FT<sup>2</sup>-HR.  
 $R_0 = 1.00$  FT.  
 $Z_0 = 1.00$  FT.  
 O2 CONC, MIN = 0.

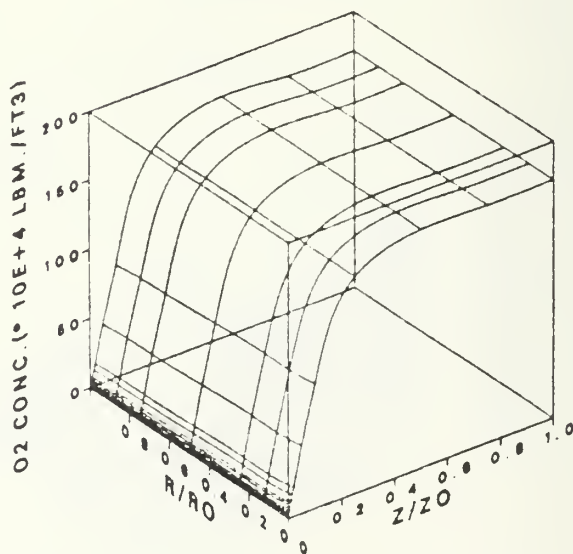


Figure 4.10 Oxygen Conc. Profile  
 with Varying Heat Flux

Heat flux was varied 4 times (500, 1000, 1500, and 2000 Btu/ft<sup>2</sup>-hr).

The relationship between the carbon temperature and the heat flux, after exposing the system to about 5 minutes of heat flux, was observed as follows:

Heat Flux (Btu/ft <sup>2</sup> -hr)	Heated Time (minutes)	Carbon Temperature (degrees F)
500	5.2	363
1000	5.1	620
1500	5.0	885
2000	4.2	1091

Heat fluxes beyond 2000 Btu/ft<sup>2</sup>-hr cause the oxygen concentration to be depleted before 5 minutes, making the data unusable for any valid comparisons.

The relationship between the oxygen concentration and heat flux, after exposing the system to approximately 5 minutes of heat flux, was observed as follows:

Heat Flux (Btu/ft <sup>2</sup> -hr)	Heated Time (minutes)	Oxygen Concentration (lbm O <sub>2</sub> /ft <sup>3</sup> )
500	5.2	$172 \times 10^{-4}$
1000	5.1	$172 \times 10^{-4}$
1500	5.0	$119 \times 10^{-4}$
2000	4.2	0

#### C. EFFECTS OF BOUNDARY CONDITIONS

Figure 4.11 shows the results of the temperature and oxygen concentration with the same initial conditions and

HEAT FLUX = 1000 BTU/FT<sup>2</sup>-HR  
 POSITION ; R/RO = 0.5  
 Z/ZO = 0.0  
 INITIAL TEMP. = 100 F

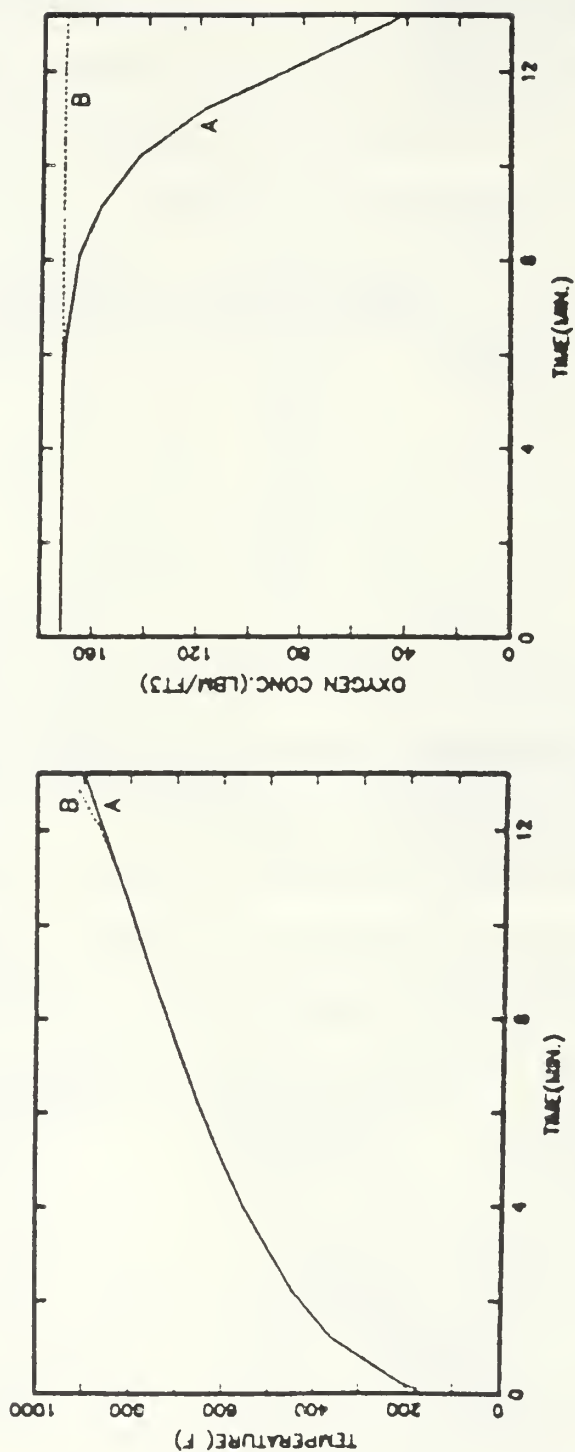


Figure 4.11 Carbon Temperature and Oxygen Conc. VS. Time  
 for a Changing Boundary Condition



boundary conditions as before, with a single exception. In case B, the boundary condition for the oxygen concentration equation at  $z/z_0 = 0.0$  was changed from a Cauchy boundary condition to a constant oxygen concentration boundary condition. As seen in Figure 4.11, carbon temperature and oxygen concentration depend on the boundary condition. The results show that whereas the case B boundary condition provides a constant supply of oxygen at  $z/z_0 = 0.0$ , the case A boundary condition leads to a decrease in oxygen, starting about  $t = 4.5$  minutes, at that boundary. For both cases (A and B), the carbon temperature remains the same until the carbon temperature reaches 860 degrees Fahrenheit which occurs at  $t = 12.0$  minutes. Thereafter, the carbon temperature for case B increases faster than the carbon temperature for case A. This may be attributed to the additional oxygen at the boundary associated with case B.

#### D. EFFECTS OF GEOMETRY

Figure 4.12 shows the carbon temperature and oxygen concentration at  $z/z_0 = 0.0$  and  $r/r_0 = 0.5$ , for three cylinders of different axial lengths. The heat flux for each case is 1000 Btu/ft<sup>2</sup>-hr. Varying the axial length of the cylinder, the carbon temperature and oxygen concentration yields different results. As shown in Figure 4.12, the carbon temperature increases with increasing axial length, while the oxygen concentration decreases with increasing axial length. These results

HEAT FLUX = 1000 BTU/FT<sup>2</sup>-HR  
 POSITION: R/RO = 0.5  
 Z/ZO = 0.0  
 INT. TEMP. = 100°F

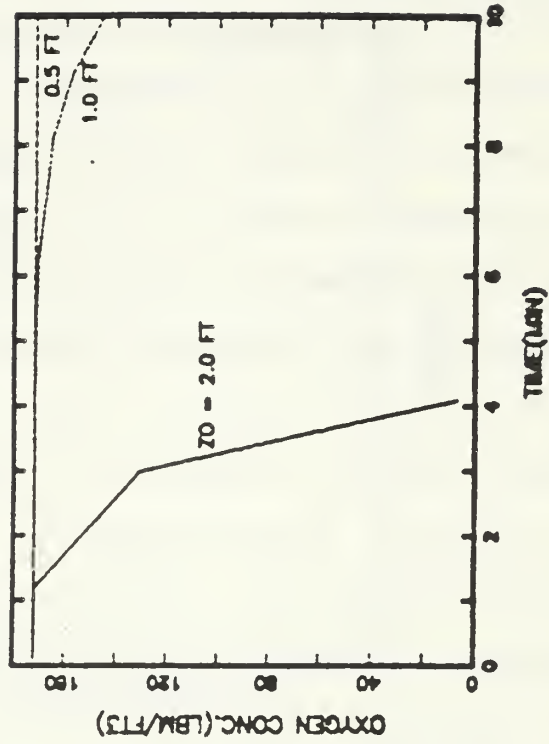
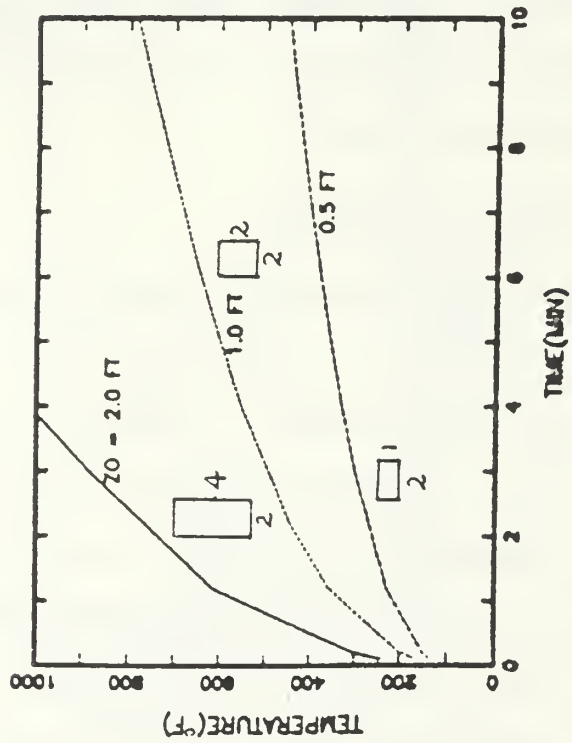


Figure 4.12 Carbon Temperature and Oxygen Conc. VS. Time for Varying the Axial Length of the Cylinder

are difficult to understand, and may indicate that the program is not performing correctly.

#### E. CONCLUSIONS AND RECOMMENDATIONS

This analysis shows that the behavior of combustion and heat transfer in a porous carbon medium is a complex process. The behavior of the system depends upon porosity, permeability, boundary conditions, initial conditions, and geometry. Some of the results of this investigation could be satisfactorily expected (the effects of the  $d/D$  ratios, and the boundary conditions), while others could not (the effects of permeability, and the effects of the geometry). The computer program developed by Lt. Martinez was used. This computer program was initially confirmed by Lt. Martinez by the model validation tests on cylinder problems with known solutions. However during this investigation, two difficulties with the computer program were encountered. First, the computer program terminates when a carbon temperature is higher than  $1300^{\circ}\text{F}$  and an oxygen concentration is less than  $10^{-7}$  lbm/ft<sup>3</sup>. This indicates that the integration algorithm was not able to perform satisfactorily when severe gradients occurred. Secondly, some results, such as the effects of permeability change and geometry change, are unexpected and infer that the program may have some errors in it.

Improvements may be realized by extending the porous carbon medium model to include:

- (1) development of an integration algorithm which is capable of performing satisfactorily over a larger range of temperatures;
- (2) a detailed investigation of the program to determine whether there are errors associated with permeability and geometric effects.

APPENDIX  
BOUNDARY CONDITIONS

Boundary conditions employed were as follows for the carbon,

$$\left. \frac{\partial T_c}{\partial r} \right|_{\frac{r}{r_0} = 0} = 0 \quad (A.1)$$

$$(1-p)(k_e) \left. \frac{\partial T}{\partial z} \right|_{\frac{z}{z_0} = 0} = -q_s'' \quad (A.2)$$

where  $q_s$  is the starting heat flux.

$$(1-p)(k_e) \left. \frac{\partial T}{\partial z} \right|_{\frac{z}{z_0} = 1} = -\sigma \epsilon (\hat{T}_c^4 - \hat{T}_\infty^4) \quad (A.3)$$

$$(1-p)(k_e) \left. \frac{\partial T}{\partial r} \right|_{\frac{r}{r_0} = 1} = \begin{cases} 0 & (1-D \text{ problems}) \\ h_r(T_c - T) + \sigma \epsilon (\hat{T}_c^4 - \hat{T}_\infty^4) & (2-D \text{ problems}) \end{cases} \quad (A.4)$$

For air,

$$\left. \frac{\partial T_a}{\partial r} \right|_{\frac{r}{r_0} = 0} = 0 \quad (A.5)$$

$$p k_a \left. \frac{\partial T_a}{\partial z} \right|_{\frac{z}{z_0} = 0} = p \rho_a C_a v (T - T_\infty) \quad (\text{A.6})$$

$$T_a \Big|_{\frac{z}{z_0} = 0} = T_\infty \quad (\text{A.7})$$

$$p k_a \left. \frac{\partial T_a}{\partial z} \right|_{\frac{z}{z_0} = 1} = - p \rho_a C_a v (T_a - T_\infty) \quad (\text{A.8})$$

$$p k_a \left. \frac{\partial T_a}{\partial r} \right|_{\frac{r}{r_0} = 1} = \begin{cases} 0 & \text{(1-D problems)} \\ h_r (T_a - T_\infty) + \sigma \epsilon (T_a^4 - T_\infty^4) & \text{(2-D problems)} \end{cases} \quad (\text{A.9})$$

For pressure,

$$\left. \frac{\partial p}{\partial r} \right|_{\frac{r}{r_0} = 0} = 0 \quad (\text{A.10})$$

$$p \Big|_{\frac{z}{z_0} = 0} = p_1 \quad (\text{A.11})$$

$$p \Big|_{\frac{z}{z_0} = 1} = p_2 \quad (\text{A.12})$$

$$\left. \frac{\partial p}{\partial r} \right|_{\frac{r}{r_0} = 1} = 0 \quad (\text{A.13})$$



Finally, for  $O_2$  concentration,

$$\left. \frac{\partial \phi}{\partial r} \right|_{\frac{r}{r_0} = 0} = 0 \quad (A.14)$$

$$p \mathcal{D}_e \left. \frac{\partial \phi}{\partial z} \right|_{\frac{z}{z_0} = 0} = v(\phi - \phi_\infty) \quad (A.15)$$

$$\phi \Big|_{\frac{z}{z_0} = 0} = \phi_\infty \quad (A.16)$$

$$p \mathcal{D}_e \left. \frac{\partial \phi}{\partial z} \right|_{\frac{z}{z_0} = 1} = v(\phi - \phi_\infty) \quad (A.17)$$

$$p \mathcal{D}_e \left. \frac{\partial \phi}{\partial r} \right|_{\frac{r}{r_0} = 1} = 0 \quad (A.18)$$

## LIST OF REFERENCES

1. Emmons, H.W., "Heat Transfer in Fire," Journal of Heat Transfer, 95, May 1973, pp. 145-151.
2. Parker, A.S., and Hottel, H.C., "Combustion Rate of Carbon," Ind. and Eng. Chem., 28, November 1936, pp. 1334-1341.
3. Arthur, J.A., "Reactions between Carbon and Oxygen," Trans. Faraday Soc., 47, 1951, pp. 164-178.
4. Koizumi, M., The Combustion of Solid Fuels in Fixed Beds, 6th Int'l Symposium on Combustion, New Haven, Ct., Proceedings, pp. 557-583, August 1945.
5. Green, D.W., and Perry, R.H., Heat Transfer with a Flowing Fluid Through Porous Media, Chem. Eng. Prog. Symp., Series No. 32, 57, 1971, pp. 61-68.
6. Anderson, C.A., and Zienkiewicz, O.C., "Spontaneous Ignition: Finite Element Solutions for Steady and Transient Conditions," Journal of Heat Transfer, 96, August 1974, pp. 398-404.
7. Kim, C.S., and Chung, P.M., "An Asymptotic, Thermo-Diffusive Ignition Theory of Porous Solids Fuels," Journal of Heat Transfer, 98, May 1976, pp. 269-275.
8. Sawyer, W.K., and Shuck, L.Z., Numerical Simulation of Mass and Energy Transfer in the Longwall Process of Underground Gasification of Coal, 4th Symposium on Numerical Simulation of Reservoir Performance, Los Angeles, California, pp. 355-370, 1976.
9. Sahota, M.S., and Pagni, P.J., "Heat and Mass Transfer in Porous Media Subject to Fires," International Journal of Heat Transfer, Vol. 22, pp. 1069-1081, 1981.
10. Saatdjian, E., and Caltagirone, J.P., "Natural Convection in a Porous Layer under the Influence of an Exothermic Decomposition Reaction," Journal of Heat Transfer, 102, November 1980, pp. 654-658.
11. Chan, Y.T., and Banerjee, S., "Analysis of Transient Three-Dimensional Natural Convection in Porous Media," Journal of Heat Transfer, 103, May 1981, pp. 242-248.

12. Vatikiotis, C., Heat Transfer Model of Flow Through a Porous Medium, Doctoral Thesis, Naval Postgraduate School, Monterey, California, 1982.
13. Martinez, B., Two-D Heat Transfer Through Porous Media with Heat Generation, Mechanical Engineer's Thesis, Naval Postgraduate School, Monterey, California, 1984.
14. Semenov, N.N., Chemical Kinetics and Chain Reactions, Clarendon Press, Oxford, 1935.
15. Frank-Kamenetskii, D.A., Diffusion and Heat Transfer in Chemical Kinetics, Plenum Press, New York, 1969.

INITIAL DISTRIBUTION LIST

	No. Copies
1. Defense Technical Information Center Cameron Station Alexandria, Virginia 22304-6145	2
2. Library, Code 0142 Naval Postgraduate School Monterey, California 93943-5100	2
3. Department Chairman, Code 69 Department of Mechanical Engineering Naval Postgraduate School Monterey, California 93943-5100	1
4. Professor David Salinas, Code 69Zc Department of Mechanical Engineering Naval Postgraduate School Monterey, California 93943-5100	5
5. Park DO Sung 1087 Soobuk 2-Dong, Euiheung-Myun Gunui-Gun, Kyungsangbuk-Do Republic of Korea 630-44	5
6. Library Officer Korea Naval Academy Jinhea-Si, Jyungsangnam-Do Republic of Korea 602	2















216881

Thesis

Pl5741

Park

c.1

Analysis of combustion of a porous medium.

216881

Thesis

Pl5741

Park

c.1

Analysis of combustion of a porous medium.





Analysis of combustion of a porous medium



3 2768 000 65596 3

DUDLEY KNOX LIBRARY c.1